for a considerable period of time. Adult human skin has an average surface area of 1.95 m^2, weighs 3.18 kg and comprises over 300 million cells. The skin is the largest organ in the human body, which provides protection against heat, cold, electromagnetic radiation and chemical damage. Indeed, skin cells are likely to have the highest frequency of exposure to nSPs. Hence, a safety evaluation of nSPs using dermal cells is essential. Based on this consideration, using the HaCaT human keratinocyte cell line as a model system, we studied the effects of various sized silica particles on cell function. Specifically, we used HaCaT cells to perform the LDH release assay to assess membrane damage induced by silica particles. We found that membrane damage was not observed in nSP300- and mSP1000-treated HaCaT cells. By contrast, LDH release increased after exposure of the cells to nSP70 in a dose-dependent manner (Figure 2). This observation suggested that membrane damage in keratinocytes increased significantly when the particle size was less than 100 nm. The decrease of particle size changes the physicochemical properties of the silica particles, such as surface area and the number of functional groups per particle weight, which are both increased [31-34]. In addition, subsequent experiments were performed at a non-toxic dose (less than 300 μg/ml) in order to exclude the toxic effects of nSP70.

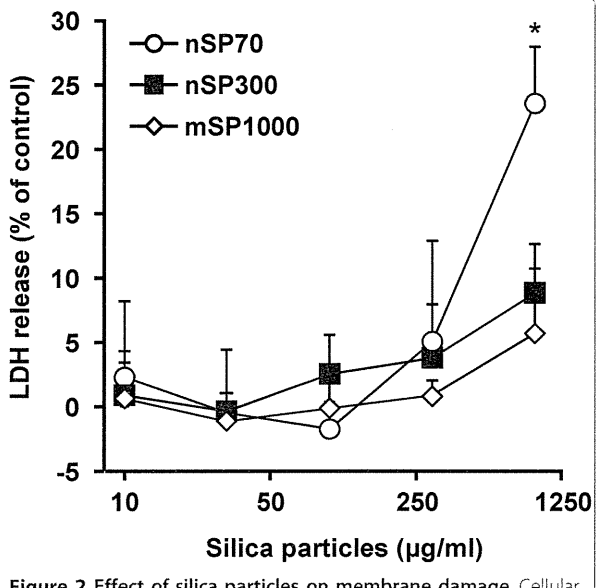

Figure 2 Effect of silica particles on membrane damage. Cellular membrane damage in HaCaT cells after incubation with nSP70 (circles), nSP300 (squares) and mSP1000 (diamonds) for 24 h was evaluated by the LDH release assay. The percentage cellular membrane damage was calculated relative to the negative (medium) controls. Data are presented as means ± SD (n = 3).*P < 0.01 vs same dose of nSP300 and mSP1000.

Some reports have indicated that intracellular generation of reactive oxygen species (ROS) is induced by nSP [35-37]. Furthermore, it has recently been reported that crystalline silica induces intracellular ROS generation *via* NADPH oxidase activation following uptake by endocytosis [38,39]. Based on these reports, ROS generation and DNA damage are an obvious means of assessing the hazard posed by nSP. Firstly, total intracellular ROS generation was measured in silica particle-treated HaCaT cells using 2'7'-dichlorodihydorofluorescein diacetate (DCFH-DA). Silica particles of all sizes were found to induce intracellular ROS generation in a dose-dependent fashion (Figure 3A). However, ROS generation by nSP70 treatment was significantly greater compared with nSP300 and mSP1000 treatment at the same particle concentration. Additionally, we confirmed that hydroxyl radicals, one of the most highly reactive ROS, were generated in HaCaT cells treated with silica particles, in particular with nSP70 (Figure 3B). Even in the 10 μg/ml-treated group, hydroxyl radical-generation effects of nSP70-treatment were 1.4 times higher than that of nSP300 and mSP1000-treated groups. These results suggested that silica particle-induced intracellular ROS generation was significantly increased by decreasing the particle size to less than 100 nm. ROS are defined as either "primary" or "secondary". Primary ROS (e.g. superoxide, O_2^-) can be generated through metabolic processes or through the activation of oxygen, which results in the formation of a reactive nucleophilic molecule of oxygen i.e., superoxide anion. These reactive species may interact with other molecules, such as redox active transition metals (e.g. iron) or enzymes, resulting in the production of "secondary" ROS (e.g. $^{\bullet}OH$), which are primary mediators of DNA damage. Consequently, we analyzed the formation of 7'8'-dihydro-8-oxodeoxyguanosine (8-OH-dG) as an indicator of ROS-induced DNA damage. When HaCaT cells were treated with various concentrations of silica particles for 3 h, 8-OH-dG levels in nSP300- and mSP1000-treated cells remained constant regardless of silica particle dose and were equal to the levels found in untreated cells (Figure 3C). By contrast, 8-OH-dG levels increased upon exposure of the cells to nSP70 in a dose-dependent manner. After treatment with nSP70 at 90 μg/ml the level of 8-OH-dG increased significantly compared with non-treated cells.

8-OH-dG is known as a major index of oxidative DNA damage related to mutagenesis, carcinogenesis and the aging process [40,41]. These reports, together with our results, suggest the possibility that nSP70 may be carcinogenic. Moreover, nSP-induced ROS may induce genotoxicity *via* DNA strand breaks, oxidative DNA damage and mutation. Indeed, DNA damage was detected in nSP70-treated HaCaT cells. In addition, nSP70-mediated DNA damage was inhibited by pre-treatment with the ROS scavenger, N-acetylcystein

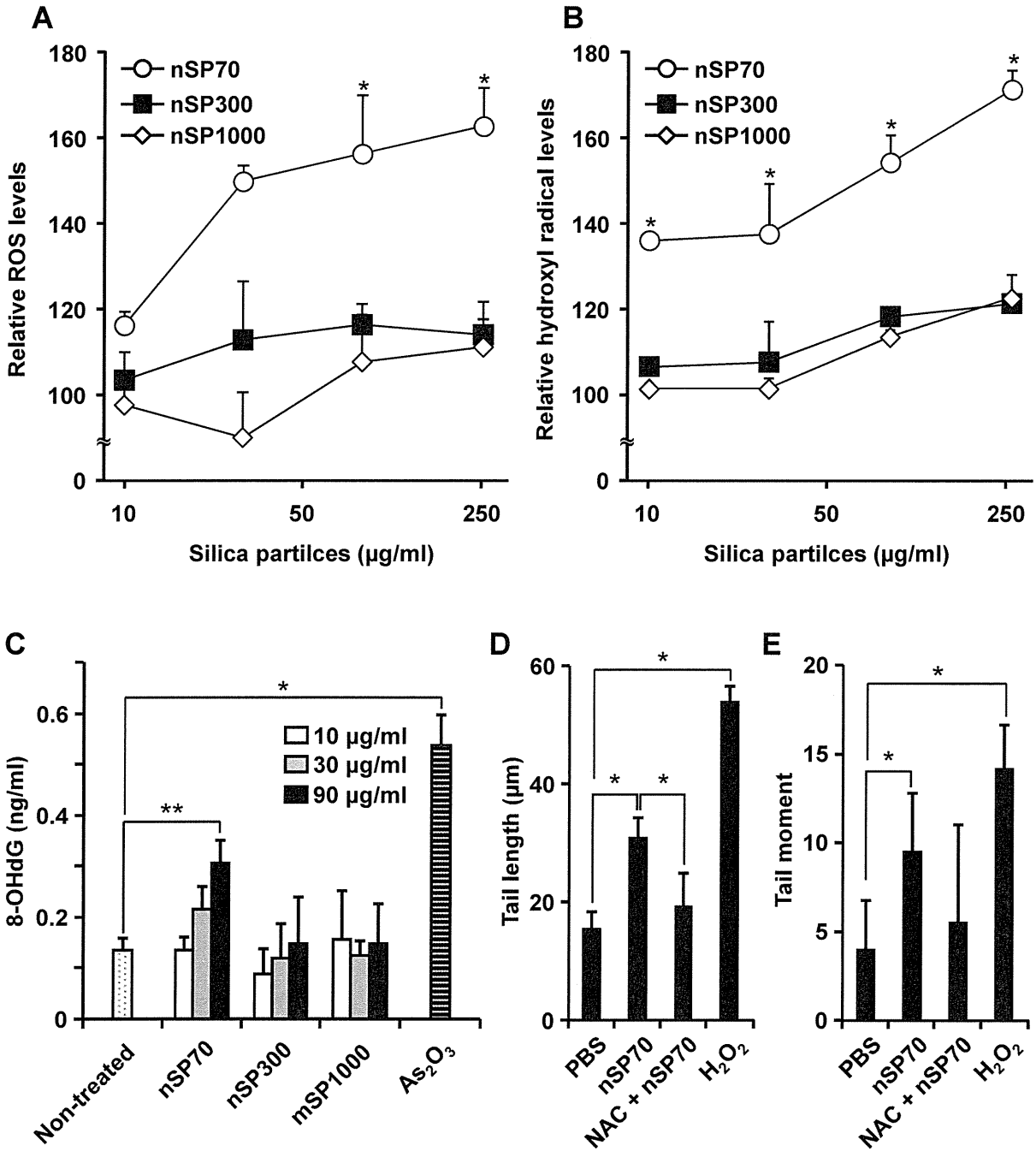

Figure 3 Detection of oxidative stress induced by silica particle treatment in HaCaT cells. Detection of total ROS and hydroxyl radical induced by silica particle treatment in HaCaT cells. HaCaT cells were incubated with various concentrations of nSP70 (circles), nSP300 (squares), and mSP1000 (diamonds) for 3 h. (**A**) Total ROS induced by treatment with silica particles were expressed as relative fluorescence units in the DCFH assay.*$P < 0.01$ vs same dose of nSP300 and mSP1000. (**B**) Hydroxyl radical was measured by hydroxyphenyl fluorescein (HPF) assay. Data shown are means ± SD (n = 3).*$P < 0.01$ vs same dose of nSP300 and mSP1000. (**C**) Detection of 8-OH-dG induced by silica particle treatment in HaCaT cells. HaCaT cells were incubated with 10, 30 or 90 mg/ml nSP70, nSP300, or mSP1000, and As_2O_3 (positive control) for 3 h. Data shown are means ± SD (n = 3). *$P < 0.01$, **$P < 0.05$. (**D and E**) Effects of ROS inhibitor on DNA strand breaks induced by silica particle treatment in HaCaT cells. HaCaT cells were pretreated with 2 mM N-acetylcystein (NAC) for 30 min (NAC + nSP70) or nSP70 alone, prior to incubation with 90 mg/ml nSP70 for 3 h. As a positive control, HaCaT cells were treated with 0.2 mM H_2O_2 for 3 h. (**D**) Column height shows the tail length. (**E**) Column height shows the tail moment. Data shown are means ± SD of at least 16 cells per sample. Results shown are representative of more than three independent experiments. *$P < 0.01$.

(NAC) (Figure 3D and 3E). From the results of the present study, we suggest that ROS play an important role in cellular responses such as nSP-induced DNA damage. However, the reason why ROS generation varies with particle size has not yet been clarified.

Fine or ultrafine particulate matter (PM), such as diesel exhaust particles or crystalline silica, often induces ROS generation that contributes to the induction of DNA damage or apoptosis. Although the mechanisms underlying the PM-induced oxidative stress response remains unclear, strong evidence supports PM phagocytosis as a stimulus for increased oxidative stress *via* NADPH oxidase activation [38,42,43]. In addition, Walee Chamulitrat *et al.* reported that HaCaT cells constitutively express Nox components Rac1, p40phox, and p67phox proteins [44]. In HaCaT skin keratinocyte cells, stimuli such as epidermal growth factor, Ca^{2+}-ionophore A23187, lysophosphatidic acid are capable of producing ROS [45-47]. Thus, one potential candidate for the nSP70-mediated DNA damage is ROS, which is produced by NADPH oxidase upon nSP70 phagocytosis. In order to assess the relationship between the uptake pathway and ROS generation, we measured the production of ROS induced by nSP70 in the presence or absence of a specific inhibitor of endocytosis. After treatment with cytochalasin D, an inhibitor of actin polymerization [48], ROS generation induced by nSP70 was measured by DCFH-DA assay. Results indicated that ROS generation induced by nSP70 was inhibited by pretreatment with cytochalasin D in a dose-dependent manner (Figure 4). Furthermore, nSP70-induced DNA damage was also significantly reduced by pretreatment with cytochalasin D (Figure 5A and 5B). These findings suggest that the silica particles entered the cells mainly through actin-mediated endocytosis, such as the macropinocytosis pathway, thereby inducing ROS generation and DNA damage. It is well-known that NADPH oxidase, which exists in the cytosol, cellular membrane and subcellular compartment membranes, becomes activated and generates ROS after ingestion of microorganisms into the phagosome and/or endosome [49-51]. Moreover, it is reported that TiO_2 particles induce IL-1ß production by NADPH oxidase-mediated ROS generation in the human macrophage cell line [52]. Likewise, NADPH oxidase exists in the cytosol and membranes of non-phagocyte cells, including HaCaT cells [44]. Additionally, it had been reported that inflammasomes are activated by actin-mediated endocytosis of crystalline silica, which lead to NADPH oxidase activation and ROS generation [38,39,53]. Consequently, in order to determine the role of NADPH oxidase in silica particle-induced ROS generation, the effects of pretreatment with the NADPH oxidase inhibitor, apocynin, a well-known NOX inhibitor [49,54], were investigated. As

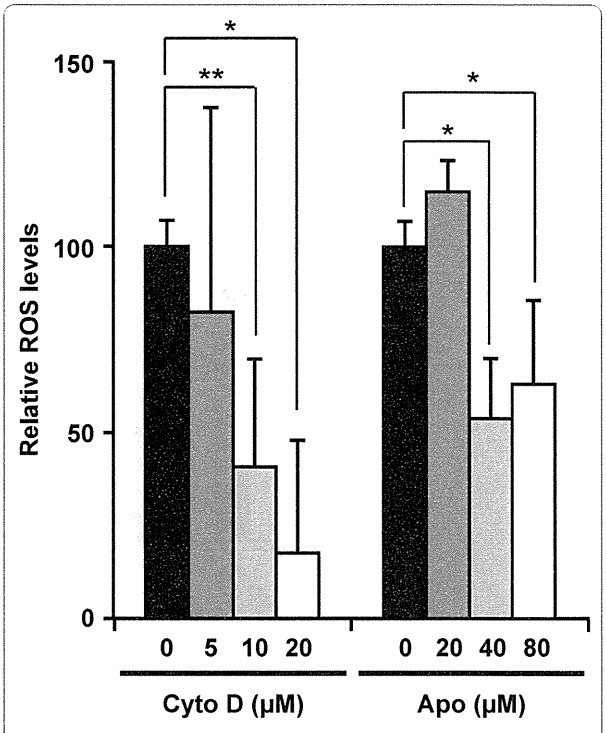

Figure 4 Effects of endocytosis and NADPH oxidase inhibitor on generation of ROS induced by silica particle treatment. HaCaT cells were pretreated with cytochalasin D or apocynin for 30 min prior to incubation with 270 mg/ml nSP70 for 3 h. ROS induced by silica particle treatment were expressed as relative fluorescence units, which means that ROS intensity of each silica particle alone and non-treatment is 100 and 0 respectively, in the DCFH assay. Data shown are means ± SD (n = 3). $^{*}P < 0.01$, $^{**}P < 0.05$.

expected, nSP70-induced ROS generation was inhibited in the presence of apocynin (Figure 4). In contrast, DNA damage induced by nSP70 was not inhibited by pretreatment with apocynin (Figure 5C and 5D). Taken together, these results suggest that nSP70-mediated DNA damage was induced by ROS generated by an unknown mechanism, and not *via* NADPH oxidase. Nox1 activation may initiate large bursts of ROS that can mediate the killing of pathogens, such as *H. pylori* [55]. Thus, NOX1 activation has been implicated in the cutaneous innate immunity to bacterial infections of the skin. A more detailed evaluation of the mechanism that underlies nSP70-mediated NOX activation is essential. Nonetheless, based on our results and the work of others, we speculate that nSP70s are treated almost like pathogens by HaCaT cells.

A number of mechanisms underlie the ability of nanoparticles to cause DNA damage. As mentioned above, a key mechanism that is often described is the ability of particles to cause the production of ROS [32,56]. One possible mechanism of particle-mediated DNA damage

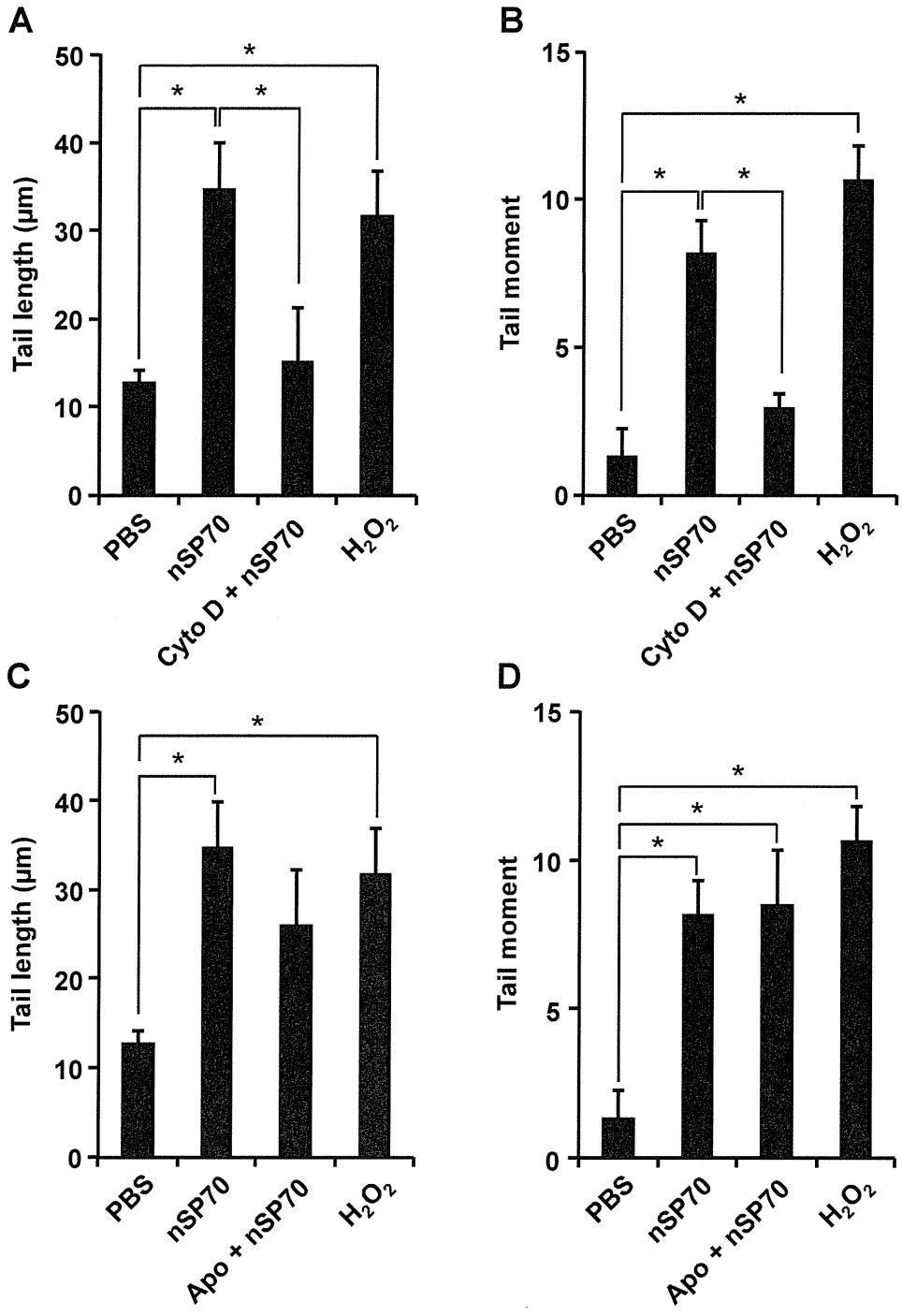

Figure 5 Effects of endocytosis and NADPH oxidase inhibitor on DNA damage by silica particle treatment. Effects of endocytosis inhibitor (**A and B**) or NADPH oxidase inhibitor (**C and D**) on DNA strand breaks induced by silica particle treatment in HaCaT cells. (**A and B**) HaCaT cells were pretreated with 10 mM cytochalasin D (Cyto D) for 30 min (Cyto D + nSP70) or nSP70 alone, prior to incubation with 90 mg/ml nSP70 for 3 h. (**C and D**) HaCaT cells were pretreated with 40 mM apocynin (Apo) for 30 min (Apo + nSP70) or nSP70 alone, prior to incubation with 90 mg/ml nSP70 for 3 h. As a positive control, HaCaT cells were treated with 0.2 mM H_2O_2 for 3 h. (**A and C**) Column height shows the tail length. (**B and D**) Column height shows the tail moment. Data shown are means ± SD of at least 16 cells per sample. Results shown are representative of more than three independent experiments. *$P < 0.01$.

is the ability of particles to stimulate target cells to produce oxidants/genotoxic compounds e.g., by affecting mitochondrial electron transport, activation of NADPH oxidase, or inducing cytochrome P450 enzymes. Our results show that nSP70-mediated DNA damage of HaCaT cells occurred *via* a mechanism that did not involve NADPH oxidase. Alternatively, transition metal ions (such as cadmium, chromium, cobalt, copper, iron, nickel, titanium and zinc) released from certain nanoparticles have the potential to cause the conversion of cellular oxygen metabolic products such as H_2O_2 and superoxide anions to hydroxyl radicals, which is one of the primary DNA damaging species. Well-known examples of the consequences of metal ion-contamination in relation to nanotoxicity have been described for carbon nanotubes. Indeed, iron contaminants in CNT have been shown to result in a substantial loss of glutathione and increased lipid peroxidation in alveolar macrophages, indicators of oxidative stress [57]. However, our data suggests that the nSPs used in this study, nSP70, nSP300 and mSP1000, were not contaminated with metal ions (data not shown). Thus, it is highly unlikely that metal ion contamination is involved in nSP70-induced DNA damage. Another hypothesis is that the size of nSPs is related to its oxidative stress. As particle size decreases, the particle unit of mass and overall surface area increases. This larger surface area enhances catalytic activity. Indeed, it has been widely reported that increased surface area of these particles increases reactivity because surface atoms have a tendency to possess high energy bonds. In order to gain stabilization, these surface bonds will readily react with other molecules [58]. The specific surface area was calculated by means of the following equation; $s = 6/d\rho$ (where s, specific surface area (m^2/g); ρ, density (g/cc); d, diameter (μm)). The specific surface area of nSP70, nSP300 and mSP1000 calculated using this equation was 43, 10 and 3 m^2/g, respectively. When specific area is considered, rather than particle concentration, the membrane damage activity of nSP70 and nSP300-treated cells shows almost the same level of LDH release per unit surface area (data not shown). In terms of ROS generation and DNA oxidation, nSP70 is more potent than nSP300. These results suggest that nSP70, which possesses a larger specific surface area compared to the counterpart micron-sized silica particles, has a much greater chance of interaction with biomolecules. Consequently, nSP70 causes direct cellular damage and promotion of oxidative stress. In addition to these hypotheses, nanoparticles may gain direct access to DNA *via* nuclear transport. However, this mechanism seems very unlikely given that the nuclear pore complex is known to be 8-30 nm in diameter, depending on cell type [59]. Nonetheless, some studies have reported that nanoparticles can penetrate the nuclear membrane, such as silica nanoparticles (40-70 nm) [60]. Detailed analysis of the mechanism of DNA damage induced by nanoparticles is currently underway. This information will be a critical determinant in the design of safer nSPs and will provide valuable information for hazard assessment of nSPs.

Here, we report the effects induced by well-dispersed amorphous silica particles (nSPs) on human keratinocyte (HaCaT) cells. In addition to our own work, other studies have shown that well-dispersed nSPs induce cytotoxicity, including LDH release, in a dose-dependent and size-dependent manner using a macrophage cell line [61,62]. On the other hands, Lin et al. reported that nSPs mediated cytotoxicity/DNA damage against A549 cells were not correlated with particle size [36]. Further, Barnes et al. reported that nSP induce no genotoxicity in fibroblast 3T3-L1 cells [63]. From the viewpoint of nSP-mediated toxicity, there is no consistency in these four reports including our findings. As mentioned above, there are a number of examples in the literature of conflicting results regarding nSPs. It has becoming increasingly evident that the physicochemical properties of nanomaterials, such as the size, shape, surface charge, fabricating method, etc, play a central role in governing their cellular uptake and subsequent physiologic consequences. Furthermore, experimental conditions, such as cell type and incubation time, are critical for the nanotoxicologic studies. Hence, given the inconsistencies it is difficult to draw the same conclusions. However, our results using well-dispersed nSPs indicated that nSPs were more cytotoxic and genotoxic against the human keratinocyte cell line HaCaT.

Conclusions

In this study, we show that nSP induce certain cellular responses, such as ROS generation and DNA damage. By contrast, their bulk-sized counterparts display a much reduced response. These different responses might be partly due to different mechanisms, such as intracellular uptake and ROS generation. We speculated that receptor-mediated uptake was involved in these phenomena and set out to identify the physicochemical properties that affect receptor endocytosis. We believe a detailed analysis of nSP-internalization will be invaluable for both hazard assessment and the design of safe nSPs.

Materials and methods

Silica particles

Suspensions of fluorescent (red-F)-labeled amorphous silica particles (Micromod Partikeltechnologie GmbH) (25 mg/ml and 50 mg/ml) were used in this study; particle size diameters were 70, 300 and 1000 nm (designated as nSP70, nSP300 and mSP1000,

respectively). Silica particle suspensions were stored in the dark at room temperature. The suspensions were sonicated for 5 min and then vortexed for 1 min immediately prior to use.

Cell Culture

The HaCaT human keratinocyte cell line was kindly provided by Dr. Inui [64], Osaka University. HaCaT cells were cultured in Dulbecco's modified Eagle's medium (D-MEM) supplemented with 10% heat-inactivated fetal bovine serum and 0.2 mM L-glutamine. The cells were grown in a humidified incubator at 37°C (95% room air, 5% CO_2).

Physicochemical examinations of silica particles

Silica particle suspensions were diluted to 0.25 mg/ml (nSP70), 0.5 mg/ml (nSP300 and mSP1000) with water or PBS, respectively and the average particle sizes were then measured using the Zetasizer Nano-ZS (Malvern Instruments Ltd). The mean size and the size distribution of silica particles were measured by a dynamic light scattering method. The size and shape of silica particles were determined using scanning electron microscopy (SEM). Each silica particle suspension was dropped on the sample stage and dried. The dried silica particles were then observed by SEM.

LDH release assay

Lactate dehydrogenase (LDH) is released from HaCaT cells exposed to nSP70, nSP300 or mSP1000. The LDH activity of the supernatant of the culture medium was determined using a commercial LDH cytotoxicity test (WAKO, Japan) according to the manufacturer's instructions. In brief, 5×10^3 cells were seeded into each well of a 96-well plate. After 24 h incubation, cells were treated with nSP70, nSP300, mSP1000 or 0.2% Tween 20 (positive control). After a further 24 h incubation period, 50 μl of medium overlying cells was used for LDH analysis. Absorption of light at 560 nm was measured using a spectrophotometer.

Detection of Reactive Oxygen Species (ROS)

The generation of total intracellular ROS was measured by monitoring the increasing fluorescence of 2'7'-dichlorofluorescein (DCF). The cell-permeant 2'7'-dichlorodihydorofluorescein diacetate (DCFH-DA; Sigma, St. Louis, MO) enters the cell where intracellular esterases cleave off the diacetate group. The resulting DCFH is retained in the cytoplasm and oxidized to DCF by ROS. Hydroxyl radical was measured by monitoring the increasing fluorescence of hydroxyphenyl fluorescein (HPF; SEKISUI MEDICAL Co., Ltd., Japan). 3×10^4 HaCaT cells were seeded into each well of a 96-well plate. After 24 h incubation, cells were treated with nSP70, nSP100, nSP300, mSP1000 or 2 mM H_2O_2 (positive control). Cells were then washed once with phenol red-free medium, and incubated in 100 μl working solution of DCFH-DA or HPF (10 μM) at 37°C for 30 min. Using the fluorescence reader (ARVO MX; Perkin Elmer, Waltham, MA), the fluorescence of DCF or HPF was monitored at the excitation and emission wavelengths of 485 nm and 530 nm or 490 nm and 515 nm, respectively.

8-Hydroxy-2-deoxyguanosine (8-OH-dG) measurement

HaCaT cells were seeded on a 100 mm dish. After 24 h, cells were treated with various concentrations of nSP70, nSP300, mSP1000, 0.2 mM H_2O_2 (positive control) or PBS (negative control). After 3 h, cellular DNA was isolated using DNeasy tissue kit (QIAGEN, Germany). Ten μg of DNA was converted to single stranded DNA by incubation with 180 U Exonuclease III (Takara Biotech., Japan) at 37°C for 1 h. The DNA was heated at 95°C for 5 min, rapidly chilled on ice, and digested to nucleosides by incubation with 0.6 U nuclease P1 (Takara) at 37°C for 1 h followed by treatment with 0.6 U *E. coli* alkaline phosphatase (Takara) for a further 1 h. The reaction mixture was centrifuged (6000 × g for 1 min) and the supernatant used for the 8-OHdG assay. The amount of 8-OHdG was measured according to the protocol of the competitive ELISA kit (8-OHdG check; Japan Institute for the Control of Aging, Japan).

Effects of inhibitor of ROS, endocytosis or NADPH oxidase on DNA strand breaks induced by silica particles

3×10^4 HaCaT cells were pretreated with 2 mM N-acetylcystein (NAC, ROS scavenger), 10 mM cytochalasin D (endocytosis inhibitor) or 40 mM apocynin (NADPH oxidase inhibitor) for 30 min prior to incubation with 90 mg/ml of nSP70 for 3 h. As a positive control, HaCaT cells were treated with 0.2 mM H_2O_2 for 3 h. DNA strand breaks were detected by alkaline comet assay according to the Comet Assay Kit (Trevigen, Gaithersburg, MD). The samples were processed according to the protocol provided in the kit. Twenty-five cells on each slide, randomly selected by fluorescence microscopy, were then analyzed using the Comet Analyzer (Youworks Corporation, Japan).

Effects of inhibitor of endocytosis, NADPH oxidase or endosomal acidification on generation of ROS induced by silica particles

HaCaT cells were pretreated with various concentration of cytochalasin D (Merck Ltd., Germany) for 30 min prior to incubation with 270 mg/ml nSP70 for 3 h. ROS induced by treatment with silica particles were expressed as relative fluorescence units in the DCFH-DA assay as described above.

Statistical analysis

Statistical comparisons between groups were performed by one-way ANOVA and a Bonferroni *post hoc* test. The level of significance was set at $P < 0.05$.

Acknowledgements

This study was supported in part by Grants-in-Aid for Scientific Research from the Ministry of Education, Culture, Sports, Science and Technology of Japan, and from the Japan Society for the Promotion of Science (JSPS). This study was also supported in part by Health Labour Sciences Research Grants from the Ministry of Health, Labor and Welfare of Japan; by Health Sciences Research Grants for Research on Publicly Essential Drugs and Medical Devices from the Japan Health Sciences Foundation; by a Global Environment Research Fund from Minister of the Environment; and by a the Knowledge Cluster Initiative; and by Food Safety Commission; and by The Nagai Foundation Tokyo; and by The Cosmetology Research Foundation; and by The Smoking Research Foundation.

Author details

[1]Graduate School of Pharmaceutical Sciences, Osaka University, 1-6 Yamadaoka, Suita, Osaka 565-0871, Japan. [2]Laboratory of Biopharamceutical Research (Pharmaceutical Proteomics), National Institute of Biomedical Innovation, 7-6-8, Saito-Asagi, Ibaraki, Osaka, 567-0085, Japan. [3]The Center for Advanced Medical Engineering and Informatics, Osaka University, 1-6, Yamadaoka, Suita, Osaka, 565-0871, Japan.

Authors' contributions

HN and TY designed the study. HN, KM, YN, STo, SK, TH and TA performed experiments. HN and TY collected and analysed data. HN and TY wrote the manuscript. KN, YA, YY, HK, NI and STs gave technical support and conceptual advice. YT supervised the all of projects. All authors discussed the results and commented on the manuscript.

Competing interests

The authors declare that they have no competing interests.

Received: 13 September 2010 Accepted: 15 January 2011
Published: 15 January 2011

References

1. Salata O: **Applications of nanoparticles in biology and medicine.** *J Nanobiotechnology* 2004, **2**:3.
2. Aiso S, Yamazaki K, Umeda Y, Asakura M, Takaya M, Toya T, Koda S, Nagano K, Arito H, Fukushima S: **Pulmonary Toxicity of Intratracheally Instilled Multiwall Carbon Nanotubes in Male Fischer 344 Rats.** *Ind Health* 2010.
3. Chen J, Dong X, Zhao J, Tang G: **In vivo acute toxicity of titanium dioxide nanoparticles to mice after intraperitioneal injection.** *J Appl Toxicol* 2009, **29**:330-337.
4. Geys J, Nemmar A, Verbeken E, Smolders E, Ratoi M, Hoylaerts MF, Nemery B, Hoet PH: **Acute toxicity and prothrombotic effects of quantum dots: impact of surface charge.** *Environ Health Perspect* 2008, **116**:1607-1613.
5. Heng BC, Zhao X, Xiong S, Ng KW, Boey FY, Loo JS: **Toxicity of zinc oxide (ZnO) nanoparticles on human bronchial epithelial cells (BEAS-2B) is accentuated by oxidative stress.** *Food Chem Toxicol* 2010, **48**:1762-1766.
6. Kocbek P, Teskac K, Kreft ME, Kristl J: **Toxicological Aspects of Long-Term Treatment of Keratinocytes with ZnO and TiO(2) Nanoparticles.** *Small* 2010, **6**:1908-1917.
7. Liu S, Xu L, Zhang T, Ren G, Yang Z: **Oxidative stress and apoptosis induced by nanosized titanium dioxide in PC12 cells.** *Toxicology* 2010, **267**:172-177.
8. Moos PJ, Chung K, Woessner D, Honeggar M, Cutler NS, Veranth JM: **ZnO particulate matter requires cell contact for toxicity in human colon cancer cells.** *Chem Res Toxicol* 2010, **23**:733-739.
9. Murray AR, Kisin E, Leonard SS, Young SH, Kommineni C, Kagan VE, Castranova V, Shvedova AA: **Oxidative stress and inflammatory response in dermal toxicity of single-walled carbon nanotubes.** *Toxicology* 2009, **257**:161-171.
10. Park EJ, Kim H, Kim Y, Yi J, Choi K, Park K: **Carbon fullerenes (C60s) can induce inflammatory responses in the lung of mice.** *Toxicol Appl Pharmacol* 2010, **244**:226-233.
11. Poland CA, Duffin R, Kinloch I, Maynard A, Wallace WA, Seaton A, Stone V, Brown S, Macnee W, Donaldson K: **Carbon nanotubes introduced into the abdominal cavity of mice show asbestos-like pathogenicity in a pilot study.** *Nat Nanotechnol* 2008, **3**:423-428.
12. Shin JA, Lee EJ, Seo SM, Kim HS, Kang JL, Park EM: **Nanosized titanium dioxide enhanced inflammatory responses in the septic brain of mouse.** *Neuroscience* 2010, **165**:445-454.
13. Takagi A, Hirose A, Nishimura T, Fukumori N, Ogata A, Ohashi N, Kitajima S, Kanno J: **Induction of mesothelioma in p53+/- mouse by intraperitoneal application of multi-wall carbon nanotube.** *J Toxicol Sci* 2008, **33**:105-116.
14. Yamashita K, Yoshioka Y, Higashisaka K, Morishita Y, Yoshida T, Fujimura M, Kayamuro H, Nabeshi H, Yamashita T, Nagano K, *et al*: **Carbon nanotubes elicit DNA damage and inflammatory response relative to their size and shape.** *Inflammation* 2010, **33**:276-280.
15. Chen Z, Meng H, Xing G, Chen C, Zhao Y, Jia G, Wang T, Yuan H, Ye C, Zhao F, *et al*: **Acute toxicological effects of copper nanoparticles in vivo.** *Toxicol Lett* 2006, **163**:109-120.
16. Duan Y, Liu J, Ma L, Li N, Liu H, Wang J, Zheng L, Liu C, Wang X, Zhao X, *et al*: **Toxicological characteristics of nanoparticulate anatase titanium dioxide in mice.** *Biomaterials* 2010, **31**:894-899.
17. Li JJ, Muralikrishnan S, Ng CT, Yung LY, Bay BH: **Nanoparticle-induced pulmonary toxicity.** *Exp Biol Med (Maywood)* 2010, **235**:1025-1033.
18. Li N, Duan Y, Hong M, Zheng L, Fei M, Zhao X, Wang J, Cui Y, Liu H, Cai J, *et al*: **Spleen injury and apoptotic pathway in mice caused by titanium dioxide nanoparticules.** *Toxicol Lett* 2010, **195**:161-168.
19. Liang G, Yin L, Zhang J, Liu R, Zhang T, Ye B, Pu Y: **Effects of subchronic exposure to multi-walled carbon nanotubes on mice.** *J Toxicol Environ Health A* 2010, **73**:463-470.
20. Sung JH, Ji JH, Yoon JU, Kim DS, Song MY, Jeong J, Han BS, Han JH, Chung YH, Kim J, *et al*: **Lung function changes in Sprague-Dawley rats after prolonged inhalation exposure to silver nanoparticles.** *Inhal Toxicol* 2008, **20**:567-574.
21. Nishimori H, Kondoh M, Isoda K, Tsunoda S, Tsutsumi Y, Yagi K: **Silica nanoparticles as hepatotoxicants.** *Eur J Pharm Biopharm* 2009, **72**:496-501.
22. Aillon KL, Xie Y, El-Gendy N, Berkland CJ, Forrest ML: **Effects of nanomaterial physicochemical properties on in vivo toxicity.** *Adv Drug Deliv Rev* 2009, **61**:457-466.
23. Hoshino A, Fujioka K, Oku T, Suga M, Sasaki YF, Ohta T, Yasuhara M, Suzuki K, Yamamoto K: **Physicochemical Properties and Cellular Toxicity of Nanocrystal Quantum Dots Depend on Their Surface Modification.** *Nano Letters* 2004, **4**:2163-2169.
24. Morishige T, Yoshioka Y, Inakura H, Tanabe A, Yao X, Narimatsu S, Monobe Y, Imazawa T, Tsunoda S, Tsutsumi Y, *et al*: **The effect of surface modification of amorphous silica particles on NLRP3 inflammasome mediated IL-1beta production, ROS production and endosomal rupture.** *Biomaterials* 2010, **31**:6833-6842.
25. Sohaebuddin SK, Thevenot PT, Baker D, Eaton JW, Tang L: **Nanomaterial cytotoxicity is composition, size, and cell type dependent.** *Part Fibre Toxicol* 2010, **7**:22.
26. Fourches D, Pu D, Tassa C, Weissleder R, Shaw SY, Mumper RJ, Tropsha A: **Quantitative nanostructure-activity relationship modeling.** *ACS Nano* 2010, **4**:5703-5712.
27. Puzyn T, Leszczynska D, Leszczynski J: **Toward the development of "nano-QSARs": advances and challenges.** *Small* 2009, **5**:2494-2509.
28. Shaw SY, Westly EC, Pittet MJ, Subramanian A, Schreiber SL, Weissleder R: **Perturbational profiling of nanomaterial biologic activity.** *Proc Natl Acad Sci USA* 2008, **105**:7387-7392.
29. Tropsha A, Golbraikh A: **Predictive QSAR modeling workflow, model applicability domains, and virtual screening.** *Curr Pharm Des* 2007, **13**:3494-3504.
30. Weissleder R, Kelly K, Sun EY, Shtatland T, Josephson L: **Cell-specific targeting of nanoparticles by multivalent attachment of small molecules.** *Nat Biotechnol* 2005, **23**:1418-1423.
31. Borm P, Klaessig FC, Landry TD, Moudgil B, Pauluhn J, Thomas K, Trottier R, Wood S: **Research strategies for safety evaluation of nanomaterials, part V: role of dissolution in biological fate and effects of nanoscale particles.** *Toxicol Sci* 2006, **90**:23-32.

32. Nel A, Xia T, Madler L, Li N: **Toxic potential of materials at the nanolevel.** *Science* 2006, 311:622-627.
33. Rahman IA, Vejayakumaran P, Sipaut SC, Ismail J, Chee KC: **Size-dependent physicochemical and optical properties of silica nanoparticles.** *Materials Chemistry and Physics* 2009, 114:328-332.
34. Xia T, Kovochich M, Brant J, Hotze M, Sempf J, Oberley T, Sioutas C, Yeh JI, Wiesner MR, Nel AE: **Comparison of the abilities of ambient and manufactured nanoparticles to induce cellular toxicity according to an oxidative stress paradigm.** *Nano Lett* 2006, 6:1794-1807.
35. Eom HJ, Choi J: **Oxidative stress of silica nanoparticles in human bronchial epithelial cell, Beas-2B.** *Toxicol In Vitro* 2009, 23:1326-1332.
36. Lin W, Huang YW, Zhou XD, Ma Y: **In vitro toxicity of silica nanoparticles in human lung cancer cells.** *Toxicol Appl Pharmacol* 2006, 217:252-259.
37. Wang F, Gao F, Lan M, Yuan H, Huang Y, Liu J: **Oxidative stress contributes to silica nanoparticle-induced cytotoxicity in human embryonic kidney cells.** *Toxicol In Vitro* 2009, 23:808-815.
38. Dostert C, Petrilli V, Van Bruggen R, Steele C, Mossman BT, Tschopp J: **Innate immune activation through Nalp3 inflammasome sensing of asbestos and silica.** *Science* 2008, 320:674-677.
39. Hornung V, Bauernfeind F, Halle A, Samstad EO, Kono H, Rock KL, Fitzgerald KA, Latz E: **Silica crystals and aluminum salts activate the NALP3 inflammasome through phagosomal destabilization.** *Nat Immunol* 2008, 9:847-856.
40. Ames BN: **Dietary carcinogens and anticarcinogens. Oxygen radicals and degenerative diseases.** *Science* 1983, 221:1256-1264.
41. Harman D: **The aging process.** *Proc Natl Acad Sci USA* 1981, 78:7124-7128.
42. Li Z, Hyseni X, Carter JD, Soukup JM, Dailey LA, Huang YC: **Pollutant particles enhanced H2O2 production from NAD(P)H oxidase and mitochondria in human pulmonary artery endothelial cells.** *Am J Physiol Cell Physiol* 2006, 291:C357-365.
43. Wang T, Chiang ET, Moreno-Vinasco L, Lang GD, Pendyala S, Samet JM, Geyh AS, Breysse PN, Chillrud SN, Natarajan V, Garcia JG: **Particulate matter disrupts human lung endothelial barrier integrity via ROS- and p38 MAPK-dependent pathways.** *Am J Respir Cell Mol Biol* 2010, 42:442-449.
44. Chamulitrat W, Stremmel W, Kawahara T, Rokutan K, Fujii H, Wingler K, Schmidt HH, Schmidt R: **A constitutive NADPH oxidase-like system containing gp91phox homologs in human keratinocytes.** *J Invest Dermatol* 2004, 122:1000-1009.
45. Goldman R, Moshonov S, Zor U: **Generation of reactive oxygen species in a human keratinocyte cell line: role of calcium.** *Arch Biochem Biophys* 1998, 350:10-18.
46. Goldman R, Moshonov S, Zor U: **Calcium-dependent PAF-stimulated generation of reactive oxygen species in a human keratinocyte cell line.** *Biochim Biophys Acta* 1999, 1438:349-358.
47. Sekharam M, Cunnick JM, Wu J: **Involvement of lipoxygenase in lysophosphatidic acid-stimulated hydrogen peroxide release in human HaCaT keratinocytes.** *Biochem J* 2000, 346(Pt 3):751-758.
48. Sampath P, Pollard TD: **Effects of cytochalasin, phalloidin, and pH on the elongation of actin filaments.** *Biochemistry* 1991, 30:1973-1980.
49. Lambeth JD: **NOX enzymes and the biology of reactive oxygen.** *Nat Rev Immunol* 2004, 4:181-189.
50. Li Q, Zhang Y, Marden JJ, Banfi B, Engelhardt JF: **Endosomal NADPH oxidase regulates c-Src activation following hypoxia/reoxygenation injury.** *Biochem J* 2008, 411:531-541.
51. Ushio-Fukai M: **Localizing NADPH oxidase-derived ROS.** *Sci STKE* 2006, 2006:re8.
52. Morishige T, Yoshioka Y, Tanabe A, Yao X, Tsunoda S, Tsutsumi Y, Mukai Y, Okada N, Nakagawa S: **Titanium dioxide induces different levels of IL-1beta production dependent on its particle characteristics through caspase-1 activation mediated by reactive oxygen species and cathepsin B.** *Biochem Biophys Res Commun* 2010, 392:160-165.
53. Fubini B, Hubbard A: **Reactive oxygen species (ROS) and reactive nitrogen species (RNS) generation by silica in inflammation and fibrosis.** *Free Radic Biol Med* 2003, 34:1507-1516.
54. Meyer JW, Schmitt ME: **A central role for the endothelial NADPH oxidase in atherosclerosis.** *FEBS Lett* 2000, 472:1-4.
55. Kawahara T, Kuwano Y, Teshima-Kondo S, Kawai T, Nikawa T, Kishi K, Rokutan K: **Toll-like receptor 4 regulates gastric pit cell responses to Helicobacter pylori infection.** *J Med Invest* 2001, 48:190-197.
56. Schins RP: **Mechanisms of genotoxicity of particles and fibers.** *Inhal Toxicol* 2002, 14:57-78.
57. Kagan VE, Tyurina YY, Tyurin VA, Konduru NV, Potapovich AI, Osipov AN, Kisin ER, Schwegler-Berry D, Mercer R, Castranova V, Shvedova AA: **Direct and indirect effects of single walled carbon nanotubes on RAW 264.7 macrophages: role of iron.** *Toxicol Lett* 2006, 165:88-100.
58. Oberdorster G, Gelein R, Johnston C, Mercer P, Corson N, Finkelstein J: **Ambient ultra fine particles: Inducers of acute Lung injury? Relationships between respiratory disease and exposure to air pollution.** ILSI Press, Washington, DC; 1998, 216-229.
59. Terry LJ, Shows EB, Wente SR: **Crossing the nuclear envelope: hierarchical regulation of nucleocytoplasmic transport.** *Science* 2007, 318:1412-1416.
60. Chen M, von Mikecz A: **Formation of nucleoplasmic protein aggregates impairs nuclear function in response to SiO2 nanoparticles.** *Exp Cell Res* 2005, 305:51-62.
61. Lison D, Thomassen LC, Rabolli V, Gonzalez L, Napierska D, Seo JW, Kirsch-Volders M, Hoet P, Kirschhock CE, Martens JA: **Nominal and effective dosimetry of silica nanoparticles in cytotoxicity assays.** *Toxicol Sci* 2008, 104:155-162.
62. Waters KM, Masiello LM, Zangar RC, Tarasevich BJ, Karin NJ, Quesenberry RD, Bandyopadhyay S, Teeguarden JG, Pounds JG, Thrall BD: **Macrophage responses to silica nanoparticles are highly conserved across particle sizes.** *Toxicol Sci* 2009, 107:553-569.
63. Barnes CA, Elsaesser A, Arkusz J, Smok A, Palus J, Lesniak A, Salvati A, Hanrahan JP, Jong WH, Dziubaltowska E, *et al*: **Reproducible comet assay of amorphous silica nanoparticles detects no genotoxicity.** *Nano Lett* 2008, 8:3069-3074.
64. Inui S, Lee YF, Haake AR, Goldsmith LA, Chang C: **Induction of TR4 orphan receptor by retinoic acid in human HaCaT keratinocytes.** *J Invest Dermatol* 1999, 112:426-431.

doi:10.1186/1743-8977-8-1
Cite this article as: Nabeshi *et al.*: Amorphous nanosilica induce endocytosis-dependent ROS generation and DNA damage in human keratinocytes. *Particle and Fibre Toxicology* 2011 8:1.

Submit your next manuscript to BioMed Central and take full advantage of:

- Convenient online submission
- Thorough peer review
- No space constraints or color figure charges
- Immediate publication on acceptance
- Inclusion in PubMed, CAS, Scopus and Google Scholar
- Research which is freely available for redistribution

Submit your manuscript at
www.biomedcentral.com/submit

BioMed Central

Laboratory of Bio-Functional Molecular Chemistry[1], Laboratory of Toxicology[2], Graduate School of Pharmaceutical Sciences, Osaka University, Osaka, Japan

Effect of 70-nm silica particles on the toxicity of acetaminophen, tetracycline, trazodone, and 5-aminosalicylic acid in mice

X. Li[1], M. Kondoh[1], A. Watari[1], T. Hasezaki[1], K. Isoda[1], Y. Tsutsumi[2], K. Yagi[1]

Received September 13, 2010, accepted October 15, 2010

Masuo Kondoh, Ph. D., Laboratory of Bio-Functional Molecular Chemistry
masuo@phs.osaka-u.ac.jp
Kiyohito Yagi, Ph. D., Laboratory of Bio-Functional Molecular Chemistry, Graduate School of Pharmaceutical Sciences, Osaka University, Suita, Osaka 565-0871, Japan
yagi@phs.osaka-u.ac.jp

Pharmazie 66: 282–286 (2011) *doi: 10.1691/ph.2011.0778*

Exposure to nano-sized particles is increasing because they are used in a wide variety of industrial products, cosmetics, and pharmaceuticals. Some animal studies indicate that such nanomaterials may have some toxicity, but their synergistic actions on the adverse effects of drugs are not well understood. In this study, we investigated whether 70-nm silica particles (nSP70), which are widely used in cosmetics and drug delivery, affect the toxicity of a drug for inflammatory bowel disease (5-aminosalicylic acid), an antibiotic drug (tetracycline), an antidepressant drug (trazodone), and an antipyretic drug (acetaminophen) in mice. Co-administration of nSP70 with trazodone did not increase a biochemical marker of liver injury. In contrast, co-administration increased the hepatotoxicity of the other drugs. Co-administration of nSP70 and tetracycline was lethal. These findings indicate that evaluation of synergistic adverse effects is important for the application of nano-sized materials.

1. Introduction

Nano-sized particles, which have a diameter of less than 100 nm, are widely used in medicine, food, and machinery. With their smaller size, the physical and chemical properties of their constituents change, so that they may be toxic, for example to the lungs or liver, even though macro-particles of the same materials are not (Byrne and Baugh 2008; Nishimori et al. 2009b). Some nano-sized particles show long-term accumulation or a wide distribution in the body (Byrne and Baugh 2008; Nishimori et al. 2009b; Xie et al. 2009; Yang et al. 2008).

Recent reports indicate that some nano-sized particles can generate reactive oxygen species (ROS) on their surfaces, leading to cellular injury (Jin et al., 2008; Sharma et al. 2007; Ye et al. 2010). There are also many drugs that cause adverse effects through the generation of ROS (Ali et al. 2002; Kovacic 2005; Xu et al. 2008). Thus, nano-sized particles might enhance the side-effects of some pharmaceutical drugs. Indeed, we have shown that 70-nm silica particles (nSP70) cause liver injury but that macro-sized silica particles with a diameter of 300 and 1000 nm do not (Nishimori et al. 2009b). Also, when co-administered to mice, nSP70 but not the macro-sized silica particles enhance the toxicity of cisplatin and paraquat (Nishimori et al. 2009a). Surprisingly, co-administration of cisplatin and nSP70 was lethal, suggesting that each chemical may have different synergistic effects in the presence of nano-sized materials.

In the current study, to clarify the influence of nano-sized materials on the adverse effects of chemicals, we assessed the toxicity in mice of 5-aminosalicylic acid (an agent for treating inflammatory bowel disease), tetracycline (a broad-spectrum antibiotic), trazodone (an antidepressant), and acetaminophen (a common antipyretic analogue) in the presence or absence of nSP70.

2. Investigations and results

Several reports indicate that 5-aminosalicylic acid, which is used to treat inflammatory bowel disease, causes liver injury and interstitial nephritis (Deltenre et al. 1999; Margetts et al. 2001). Administration of 5-aminosalicylic acid caused an increase in ALT, AST and BUN levels (Fig. 1). Also, nSP70 dose-dependently elevated ALT and AST levels. Co-treatment with 5-aminosalicylic acid and nSP70 resulted in higher levels of ALT and AST than nSP70 alone. In contrast, changes in BUN levels in response to 5-aminosalicylic acid were not affected by nSP70.

Next, we investigated effect of nSP70 on tetracycline, a broad-spectrum antibiotic. As shown in Fig. 2A and 2B, administration of tetracycline did not elevate biochemical markers for liver injury. In contrast, co-administration with nSP70 resulted in the synergistic induction of liver injury. However, nSP70 alone did not cause kidney injury. Importantly, co-administration of 30 and 50 mg/kg nSP70 with tetracycline resulted in the death of 1 of 4 and 2 of 4 mice, respectively.

Finally, we investigated effect of nSP70 on toxicity of the antidepressant trazodone and the antipyretic analgesic acetaminophen. We found that nSP70 did not have a synergistic effect on the toxicity of trazodone (Fig. 3). In contrast, co-administration of acetaminophen with nSP70 caused synergistic liver injury (Fig. 4).

3. Discussion

In this study, we showed that nSP70 synergistically enhance the toxicity of 5-aminosalicylic acid, tetracycline, and acetaminophen but not trazodone. To avoid direct interac-

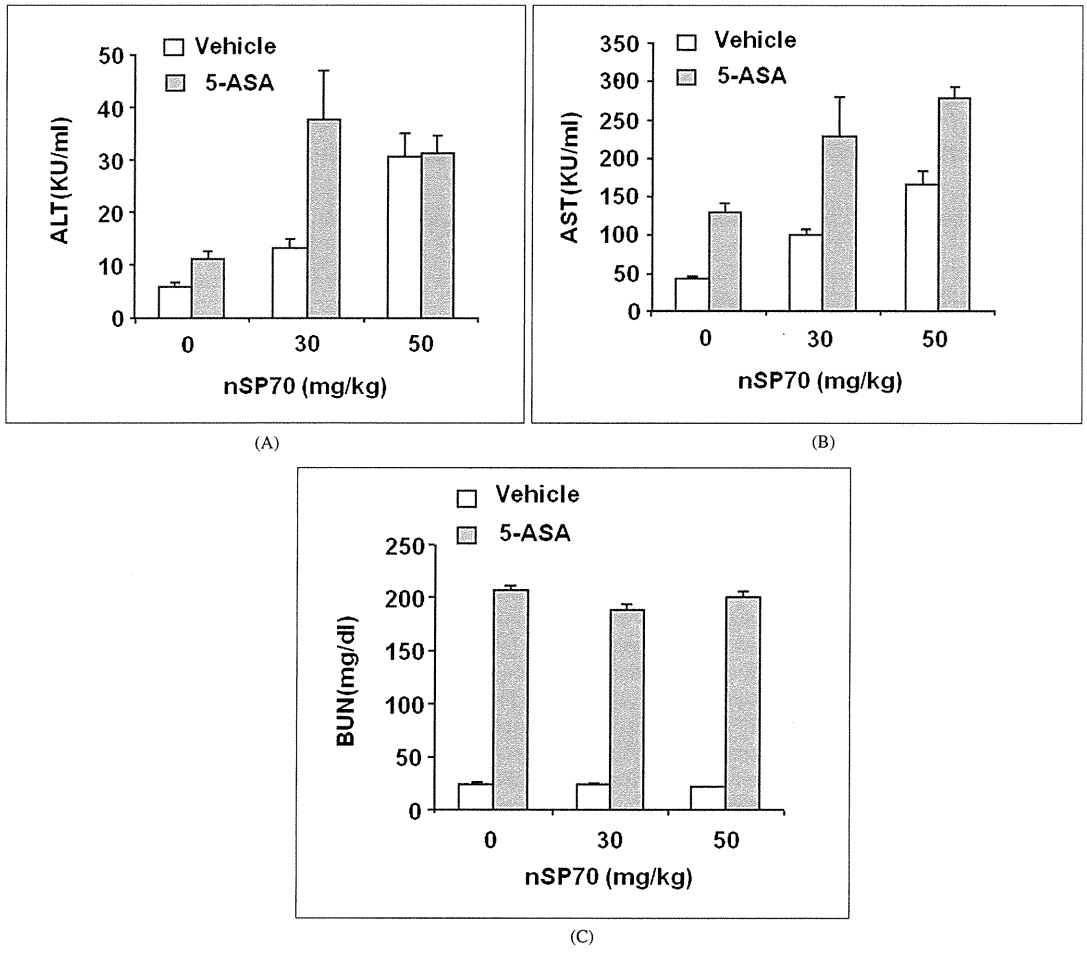

Fig. 1: Effect of nSP70 on 5-aminosalicylic acid (5-ASA)-induced toxicity Mice were injected intraperitoneally with 5-ASA at 0 (open column) or 500 mg/kg (gray column) and intravenously with nSP70 at the indicated doses. After 24 h, the serum was collected. Shown are the levels of ALT (A), AST (B), and BUN (C). Data are means ± SEM (n = 4)

tions between nSP70 and chemicals in their administration and absorption, nSP70 and chemicals were administered intravenously and intraperitoneally, respectively. Administration of nSP70 alone has been shown to cause liver injury but not kidney injury (Nishimori et al. 2009b). Also, in this study, nSP70 did not enhance kidney injury induced by 5-aminosalicylic acid or tetracycline, two drugs known to be nephrotoxic (Grisham et al. 1992; Kunin 1971). The renal toxicity of cisplatin, another nephrotoxic chemical, was unaffected by nSP70 (Nishimori et al. 2009a). Like 5-aminosalicylic acid, tetracycline, and acetaminophen (Chun et al. 2009; Herzog and Leuschner 1995; Kunin 1971), nSP70 is hepatotoxic (Nishimori et al. 2009b), and we showed here that its co-administration synergistically enhanced liver injury. These findings indicate that nSP70 may enhance the toxicity of certain chemicals. Therefore, it will be important to assess the tissue-specific risk of nano-sized materials.

The nSP70 particles had a lethal effect when combined with tetracycline. The 50% lethal dose of tetracycline is 318 mg/kg by intraperitoneal injection in mice. A previous report showed that 100 mg/kg nSP70 is lethal in 100% of mice (Nishimori et al. 2009b). A single injection of tetracycline (100 mg/kg) or nSP70 (30 or 50 mg/kg) alone was not lethal in this study but a combination of the two was. Co-administration of cisplatin and nSP70 showed a similar synergistic lethal effect. This could be due to an interaction between nSP70 and serum albumin. Tetracycline in the bloodstream can bind to albumin (Popov et al. 1972; Powis 1974). Likewise, serum albumin adsorbs onto nano-sized silica particles (Dutta et al. 2007). When injected intravenously, 100-nm anionized albumin-modified liposomes are taken up by hepatic endothelial cells and Kupffer cells (Kamps et al. 1997), which normally clear chemically modified albumin (Jansen et al. 1991). Thus, tetracycline-bound serum albumin may adsorb onto nSP70, causing it to be taken up by the hepatic endothelial cells and Kupffer cells in the liver where it may accumulate and cause lethal liver damage.

Indirect interactions between chemicals and nano-sized particles mediated by serum albumin may be useful for estimating the toxicity of nano-sized materials. In this study, co-treatment of mice with nSP70 (50 mg/kg) and tetracycline decreased BUN levels compared to tetracycline alone or nSP70 (30 mg/kg) and tetracycline. A similar decrease in BUN levels

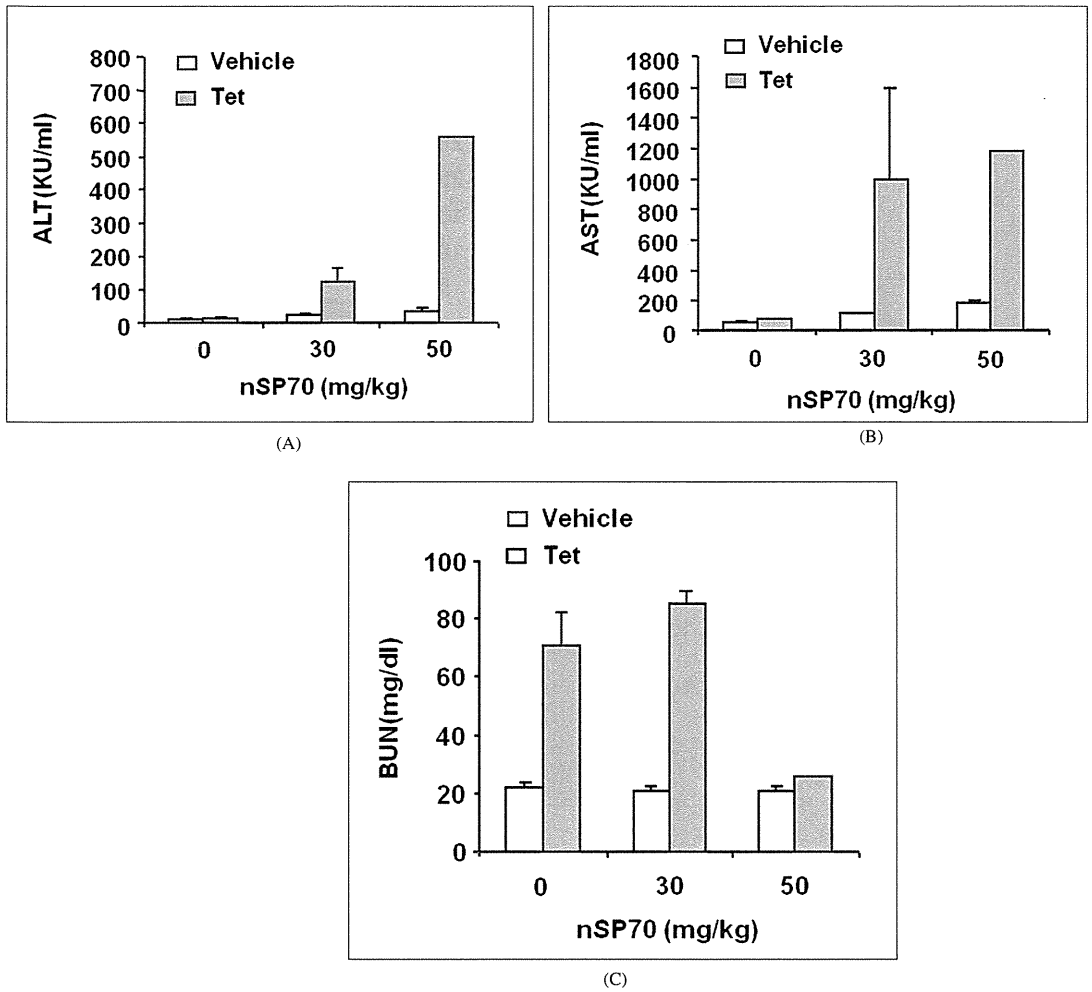

Fig. 2: Effect of nSP70 on tetracycline (Tet)-induced toxicity Mice were injected intraperitoneally with Tet at 0 (open column) or 100 mg/kg (gray column) and intravenously with nSP70 at the indicated doses. After 24 h, the serum was collected. Shown are the levels of ALT (A), AST (B), and BUN (C). One of 4 mice died when co-treated with nSP70 (30 mg/kg) and Tet (100 mg/kg), and 2 of 4 mice died when co-treated with nSP70 (50 mg/kg) and Tet (100 mg/kg). Data are means or means ± SEM (n = 2–4)

was also reported in mice co-treated with nSP70 and cisplatin (Nishimori et al. 2009a). However, the mechanism by which these decrease the BUN level remains to be determined.

In conclusion, we found that nSP70 cause synergistic toxicity when combined with some clinically used drugs, although the synergistic effects differ between chemicals. One combination was lethal, and the others resulted in tissue injury. These studies suggest that evaluation of possible synergistic adverse effects with pharmaceutical drugs may be important for assessing the safety of nano-sized particles.

4. Experimental

4.1. Materials

The nSP70 nanoparticles were obtained from Micromod Partikeltechnologie GmnH (Rostock, Germany). The mean diameter of the particles, as analyzed by a Zetasizer (Sysmex Co., Kobe, Japan), was 55.7 nm, and the particles were spherical and nonporous. The particles were stored at 25 mg/ml as an aqueous suspension. The suspensions were thoroughly dispersed by sonication before use and diluted in water. An equal volume of solution was injected for each treatment. Acetaminophen, tetracycline, and trazodone were dissolved in saline solution, and 5-aminosalicylic acid was suspended in 1% sodium salt of carboxy methyl cellulose. All reagents were of research grade.

4.2. Animals

Eight-week-old BALB/c male mice were purchased from Shimizu Laboratory Supplies Co., Ltd. (Kyoto, Japan). Mice were maintained in controlled environment (23 ± 1.5 °C; 12-h light/12-h dark cycle) with free access to standard rodent chow and water. The mice were given 1 week to adapt before experiments. All of the experimental protocols complied with the ethical guidelines of the Graduate School of Pharmaceutical Sciences, Osaka University.

4.3. Biochemical analysis

Serum alanine aminotransferase (ALT), aspartate aminotransferase (AST), and blood urea nitrogen (BUN) were measured using commercially available kits according to the manufacturer's protocols (WAKO Pure Chemical, Osaka, Japan).

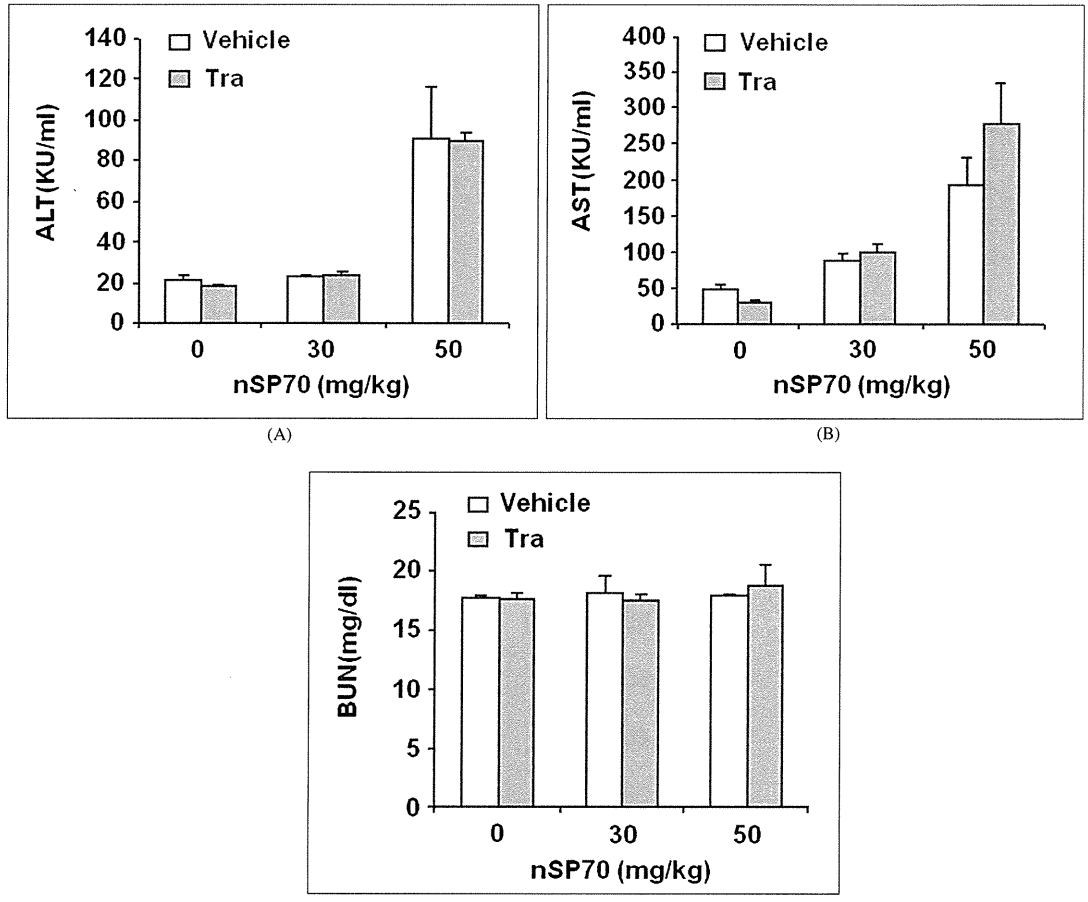

Fig. 3: Effect of nSP70 on trazodone (Tra)-induced toxicity Mice were injected intraperitoneally with Tra at 0 (open column) or 100 mg/kg (gray column) and intravenously with nSP70 at 30 or 50 mg/kg. After 24 h, the serum was collected. Shown are the levels of ALT (A), AST (B), and BUN (C). Data are means ± SEM (n = 4)

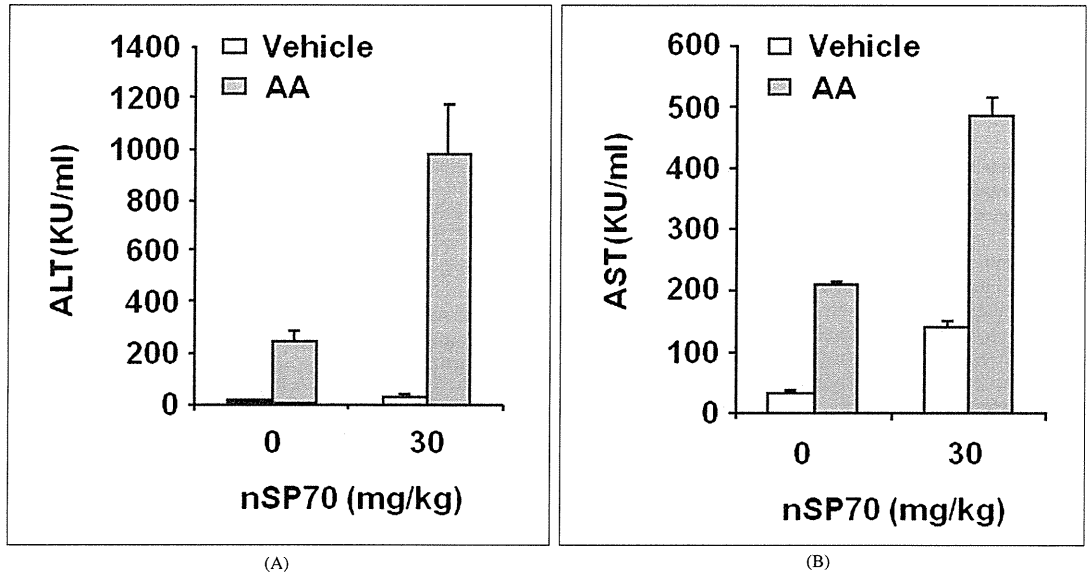

Fig. 4: Effect of nSP70 on acetaminophen (AA)-induced toxicity Mice were injected intraperitoneally with AA at 0 (open column) or 500 mg/kg (gray column) and intravenously with nSP70 (30 mg/kg). After 24 h, the serum was collected. Shown are the levels of ALT (A) and AST (B). Data are means ± SEM (n = 4)

Acknowledgements: The authors thank all members of our laboratory for their useful comments and discussion. This study was supported by a grant from the Ministry of Health, Labor, and Welfare of Japan.

References

Ali MM, Frei E, Straub J, Breuer A Wiessler M (2002) Induction of metallothionein by zinc protects from daunorubicin toxicity in rats. Toxicology 179: 85–93.

Byrne JD Baugh JA (2008) The significance of nanoparticles in particle-induced pulmonary fibrosis. Mcgill J Med 11: 43–50.

Chun LJ, Tong MJ, Busuttil RW Hiatt JR (2009) Acetaminophen hepatotoxicity and acute liver failure. J Clin Gastroenterol 43: 342–349.

Deltenre P, Berson A, Marcellin P, Degott C, Biour M Pessayre D (1999) Mesalazine (5-aminosalicylic acid) induced chronic hepatitis. Gut 44: 886–888.

Dutta D, Sundaram SK, Teeguarden JG, Riley BJ, Fifield LS, Jacobs JM, Addleman SR, Kaysen GA, Moudgil BM Weber TJ (2007) Adsorbed proteins influence the biological activity and molecular targeting of nanomaterials. Toxicol Sci 100: 303–315.

Grisham MB, Ware K, Marshall S, Yamada T Sandhu IS (1992) Prooxidant properties of 5-aminosalicylic acid. Possible mechanism for its adverse side effects. Dig Dis Sci 37: 1383–1389.

Herzog R Leuschner J (1995) Experimental studies on the pharmacokinetics and toxicity of 5-aminosalicylic acid-O-sulfate following local and systemic application. Arzneimittelforschung 45: 300–303.

Jansen RW, Molema G, Harms G, Kruijt JK, van Berkel TJ, Hardonk MJ Meijer DK (1991) Formaldehyde treated albumin contains monomeric and polymeric forms that are differently cleared by endothelial and Kupffer cells of the liver: evidence for scavenger receptor heterogeneity. Biochem Biophys Res Commun 180: 23–32.

Jin CY, Zhu BS, Wang XF Lu QH (2008) Cytotoxicity of titanium dioxide nanoparticles in mouse fibroblast cells. Chem Res Toxicol 21: 1871–1877.

Kamps JA, Morselt HW, Swart PJ, Meijer DK Scherphof GL (1997) Massive targeting of liposomes, surface-modified with anionized albumins, to hepatic endothelial cells. Proc Natl Acad Sci U S A 94: 11681–11685.

Kovacic P (2005) Role of oxidative metabolites of cocaine in toxicity and addiction: oxidative stress and electron transfer. Med Hypotheses 64: 350–356.

Kunin CM (1971) Hepatorenal toxicity of tetracycline. Minn Med 5: 532–533.

Margetts PJ, Churchill DN Alexopoulou I (2001) Interstitial nephritis in patients with inflammatory bowel disease treated with mesalamine. J Clin Gastroenterol 32: 176–178.

Nishimori H, Kondoh M, Isoda K, Tsunoda S, Tsutsumi Y Yagi K (2009a) Influence of 70 nm silica particles in mice with cisplatin or paraquat-induced toxicity. Pharmazie 64 : 395–397.

Nishimori H, Kondoh M, Isoda K, Tsunoda S, Tsutsumi Y Yagi K (2009b) Silica nanoparticles as hepatotoxicants. Eur J Pharm Biopharm 72: 496–501.

Popov PG, Vaptzarova KI, Kossekova GP Nikolov TK (1972) Fluorometric study of tetracycline-bovine serum albumin interaction. The tetracyclines-a new class of fluorescent probes. Biochem Pharmacol 21: 2363–2372.

Powis G (1974) A study of the interaction of tetracycline with human serum lipoproteins and albumin. J Pharm Pharmacol 26: 113–118.

Sharma CS, Sarkar S, Periyakaruppan A, Barr J, Wise K, Thomas R, Wilson BL Ramesh GT (2007) Single-walled carbon nanotubes induces oxidative stress in rat lung epithelial cells. J Nanosci Nanotechnol 7: 2466–2472.

Xie G, Sun J, Zhong G, Shi L Zhang D (2009) Biodistribution and toxicity of intravenously administered silica nanoparticles in mice. Arch Toxicol, in press.

Xu JJ, Henstock PV, Dunn MC, Smith AR, Chabot JR de Graaf D (2008) Cellular imaging predictions of clinical drug-induced liver injury. Toxicol Sci 105: 97–105.

Yang ST, Wang X, Jia G, Gu Y, Wang T, Nie H, Ge C, Wang H Liu Y (2008) Long-term accumulation and low toxicity of single-walled carbon nanotubes in intravenously exposed mice. Toxicol Lett 181: 182–189.

Ye Y, Liu J, Xu J, Sun L, Chen M Lan M (2010) Nano-SiO2 induces apoptosis via activation of p53 and Bax mediated by oxidative stress in human hepatic cell line. Toxicol *In Vitro* 24: 751–758.

Laboratory of Bio-Functional Molecular Chemistry[1], Laboratory of Toxicology and Safety Science[2], Graduate School of Pharmaceutical Sciences[3], Osaka University, Suita; Laboratory of Biopharmaceutical Research (Pharmaceutical Proteomics), National Institute of Biomedical Innovation, Ibaraki, Osaka, Japan

Effect of surface charge on nano-sized silica particles-induced liver injury

K. ISODA[1], T. HASEZAKI[1], M. KONDOH[1], Y. TSUTSUMI[2,3], K. YAGI[1]

Received October 5, 2010, accepted November 11, 2010

Dr Kiyohito Yagi, Laboratory of Bio-Functional Molecular Chemistry, Graduate School of Pharmaceutical Sciences, Osaka University, Suita, Osaka 565-0871, Japan
yagi@phs.osaka-u.ac.jp

Pharmazie 66: 278–281 (2011) *doi: 10.1691/ph.2011.0808*

Nanomaterials are used frequently in microelectronics, cosmetics and sunscreen, and research for the development of nanomaterial-based drug delivery systems is promising. We previously reported that the intravenous administration of unmodified silica particles with a diameter of 70 nm (SP70) caused hepatic injury. Here, we examined the acute hepatic toxicity of SP70 modified with amino group (SP70-N) or carboxyl group (SP70-C). When administered intravenously into mice, SP70-N and SP70-C dose-dependently increased the serum level of alanine aminotransferase (ALT). However, the toxicity levels of surface charge-modified silica particles were much less weaker than the level of unmodified particles. When SP70 was repeatedly administered at 40 mg/kg twice a week for 4 weeks into mice, the hydroxyproline content of the liver significantly increased. Azan staining of the liver section indicated the extensive fibrosis. To the contrary, the repeated administration of SP70-N or SP70-C at 60 mg/kg twice a week for 4 weeks into mice did not cause the hepatic fibrosis. These findings suggest that the surface charge of nanomaterials could change their toxicity.

1. Introduction

Recently, the scientific, medical, and technical applications of nanomaterials have greatly increased. Nanomaterials are frequently used in microelectronics, cosmetics and sunscreen, and their potential use in drug-delivery systems is being investigated (Dobson 2006). Nanomaterials have unique physicochemical qualities as compared to micromaterials in regard to size, surface structure, solubility, and aggregation. Thus, the reduction in particle size from the micro- to nanoscale is beneficial for many industrial and scientific applications. However, nanomaterials have potential toxicity that is not found in micromaterials, and it is, therefore, essential to understand the biological activity and potential toxicity of nanomaterials (Warheit et al. 2008).

The physical properties of nanomaterials are changed by the modification of their surface charge, which extends their possible applications. For example, charge-modified dendrimers are expected to have applications in drug-delivery systems. The physical properties and the toxicity of carbon nanotubes change based on the surface charge (Smith et al. 2009), as do the pharmacokinetics of liposomes. Future research will undoubtedly lead to expanded applications of surface-modified nanomaterials, however, little has been reported on their toxicity.

Silica nanoparticles have been applied to diagnostic measures and drug delivery methods. Intraperitoneal administration of silica nanoparticles results in the biodistribution of the nanoparticles to diverse organs, such as the liver, kidney, spleen and lung (Kim et al., 2006). We previously found that nano-size silica particles with a diameter of 70 nm caused liver injury, while micro-size particles with a diameter of 300 or 1000 nm did not (Nishimori et al. 2009a, b). In the present study, we examined the hepatic toxicity of surface charge-modified silica nanoparticles.

2. Investigations, results and discussion

The surface modification technology has been developed in the field of nanotechnology (Schiestel et al. 2004), and many nanomaterials with new functions will be produced for cosmetics and medicinal use. Thus, it should be important to investigate the effect of surface charge of nanomaterials on living body.

We initially examined the acute toxicity of 70-nm diameter silica nanoparticles (SP70) modified with amino group (SP70-N) or carboxyl group (SP70-C) at the maximal dose of 100 mg/kg. Intravenous injection of 50 mg/kg of unmodified SP70 was lethal in mice (Fig. 1A). The acute liver toxicity of SP70-N and SP70-C increased in a dose-dependent manner (Fig. 1B, C). Intravenous injection of SP70-C was lethal in all mice at 100 mg/kg and was often lethal at 80 and 60 mg/kg. SP70-C was more toxic than SP70-N. We examined the hepatic injury caused by 40 mg/kg of unmodified SP70 and 60 mg/kg of modified SP70 (SP70-C and SP70-N). The hematoxylin-eosin staining of liver tissue from mice injected with the silica nanoparticles is shown in Fig. 2A–D. The liver injury caused by SP70 was more extensive than that caused by SP70-C and SP70-N. Significant increase in the levels of BUN, a biochemical marker of kidney injury, was not observed in mice that received the nanoparticles (Fig. 3). The less amount of unmodified SP70 induced significant liver damage than the surface-modified silica particles. Thus, the

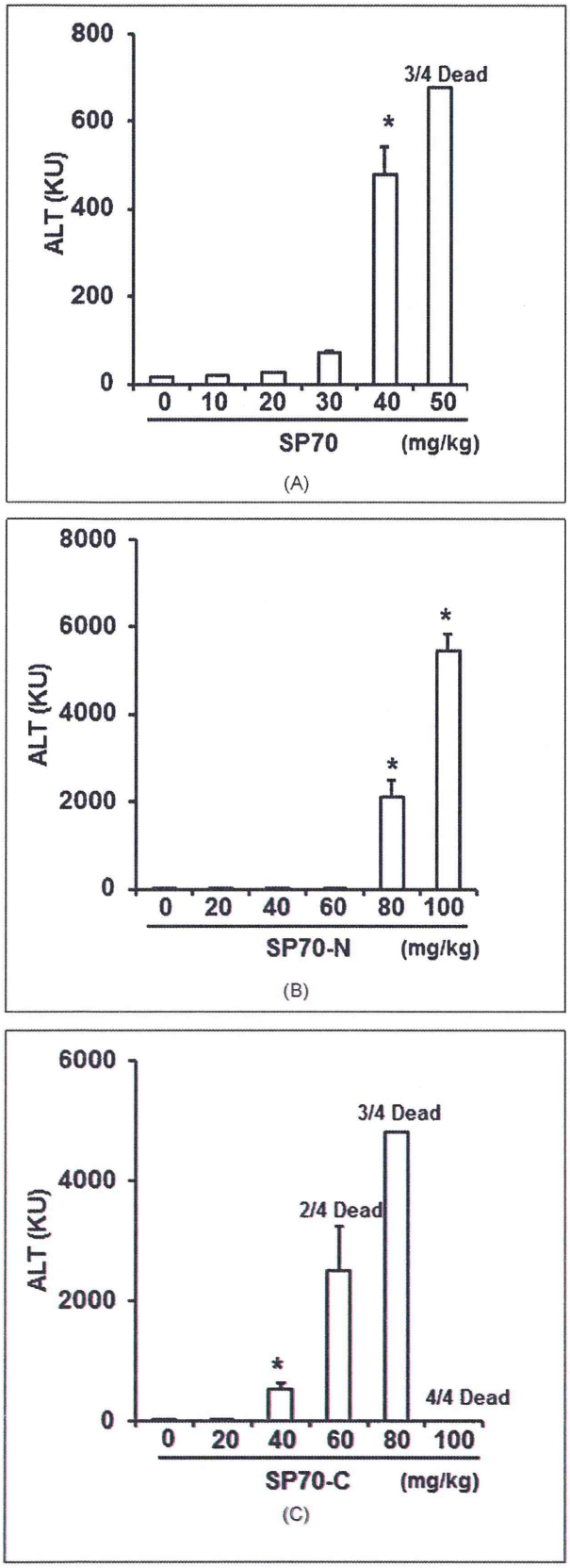

Fig. 1: Acute liver toxicity of SP70-N and SP70-C. SP70 (A), SP70-N (B) and SP70-C (C) were intravenously administered at the indicated doses. At 24 h after administration, blood was collected, and the resultant serum was used for the ALT assay. Data are means ± SEM (n = 4). *$p < 0.05$ as compared to the vehicle-treated group.

modification of the surface charge decreased the amount of acute hepatic injury caused by silica nanoparticles.

We then examined the chronic liver injury caused by 60 mg/kg of SP70-C or SP70-N as compared to 30 mg/kg of SP70. Nanoparticles were intravenously injected into mice twice a week for 4 weeks. We assessed the presence of liver fibrosis, because it is a symptom of chronic liver injury. We determined the hepatic hydroxyproline contents in the silica nanoparticle–treated mice (Fig. 4A). SP70, but not SP70-N or SP70-C, significantly increased the hepatic hydroxyproline content by 3.5-fold over the control value. Moreover, collagen, which accumulates in the fibrotic liver, was stained with Azan reagent, and blue-stained regions were observed in SP70-treated, but not SP70-C- and SP70-N-treated, liver sections (Fig. 4B-E). Thus, the chronic administration of SP70-C and SP70-N did not cause hepatic fibrosis in mice.

In this study we found that the surface modification of nanosilica particles with amino group and carboxyl group attenuated liver toxicity. We suspect that this decreased toxicity is due to a decrease in the amount of silica nanoparticles that accumulate in the liver. Oku et al. (1996) reported that the accumulation of liposomes in the liver changed depending on the surface charge of liposomes. Although we confirmed the presence of SP70-N, SP70-C and SP70 in the electron micrograph (data not shown), we were unable to compare the accumulative amounts in the liver. Therefore, an analysis of the accumulative amount of the silica nanoparticles in the liver is necessary in future studies.

The surface charge of nanoparticles might change the pharmacokinetics *in vivo*; for instance, the silica nanoparticles with a positive surface charge have increased paracellular permeability (Lin et al. 2007). Moreover, the phagocytosis of liposomes by hepatic Kupffer cells was promoted by a positive surface charge (Schiestel et al. 2004). We previously reported that the inhibition of phagocytosis by Kupffer cells increased the toxicity of nanosilica particles (Nishimori et al. 2009a). Therefore, it is thought that the nanoparticles with a positive surface charge have decreased hepatic toxicity due to increased phagocytosis by liver Kupffer cells.

This report is the first to indicate that altering the surface charge of nanomaterials changes their toxicity. Further studies based on these data will provide useful information regarding the safety of the nanomaterials.

3. Experimental

3.1. Materials

Silica particles with a diameter of 70 nm were obtained from Micromod Partikeltechnologie GmbH (Rostock, Germany). Silica particles with a diameter of 70 nm that were modified with the amino group or the carboxyl group were obtained from Micromod Partikeltechnologie GmbH (Rostock, Germany). The size distribution of the particles was analyzed using a Zetasizer (Sysmex Co., Kobe, Japan), and the mean diameters were 61.5 and 70.5 nm, respectively. The electric charge of the particles, also measured using the Zetasizer, was found to be –19.7 and –52.4 mV, respectively. The particles were spherical and nonporous and were stored at 25 mg/mL in an aqueous suspension. The suspensions were thoroughly dispersed by sonication before use and then diluted in ultrapure water. All reagents used were of research grade.

3.2. Animals

Eight-week-old BALB/c male mice were purchased from Shimizu Laboratory Supplies Co., Ltd. (Kyoto, Japan) and were maintained in a controlled environment (23 ± 1.5 °C; 12-h light/dark cycle) with access to standard rodent chow and water *ad libitum*. The mice were left to adapt to the new environment for 1 week before commencing with the experiment. Mice that received a single treatment of silica nanoparticles were anesthetized for sacrificing 24 h after intravenous injection. Mice in the frequent treatment group received intravenous administration of silica nanoparticles twice a week for 4 weeks. The experimental protocols conformed to the ethical guidelines of the Graduate School of Pharmaceutical Sciences, Osaka University.

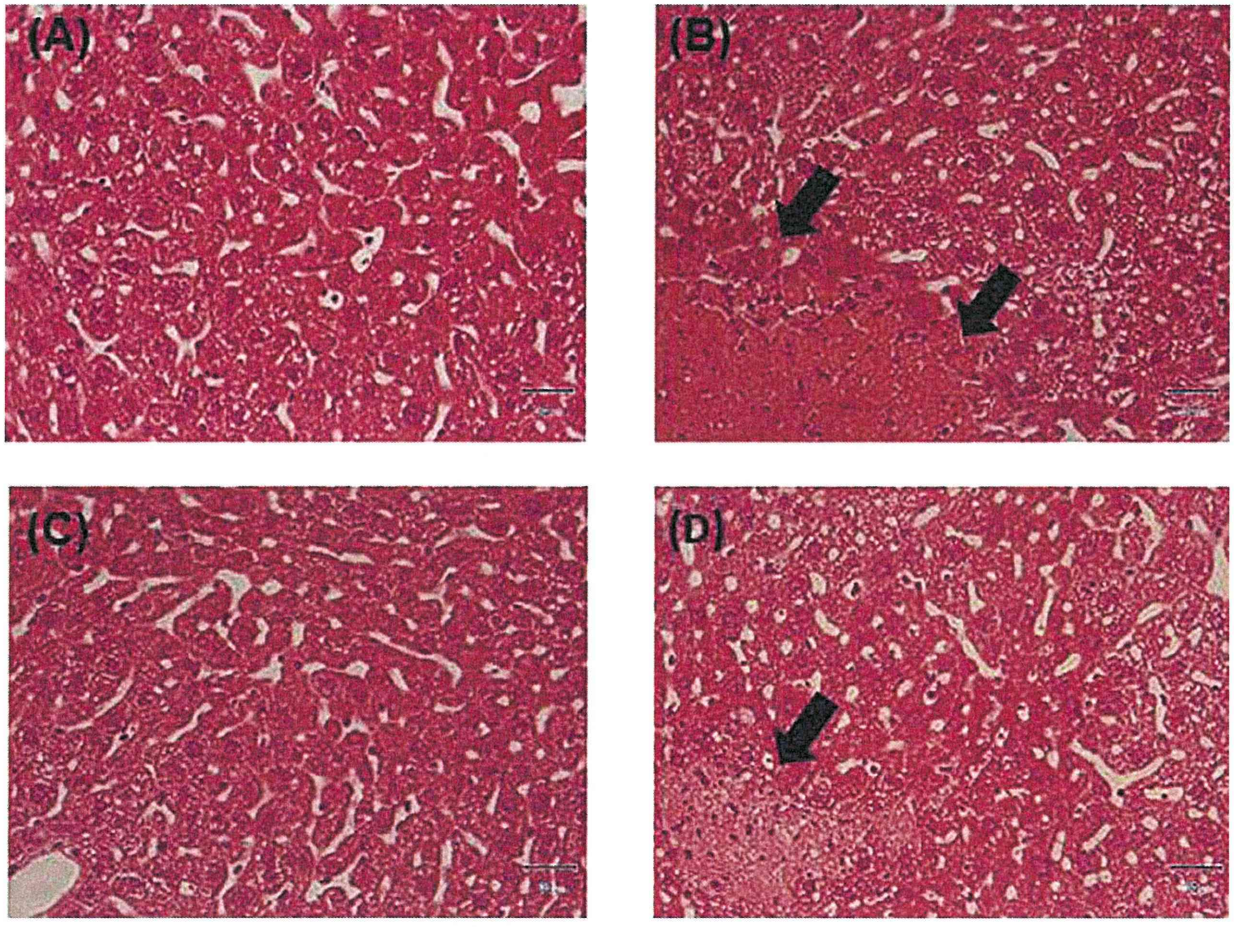

Fig. 2: Hematoxylin and eosin staining of the liver sections. Twenty-four h after administration, the liver was excised from the mice treated with vehicle (A), SP70 (B), SP70-N (C) or SP70-C (D) and fixed with 4% paraformaldehyde. Tissue sections were stained with hematoxylin and eosin and observed under a microscope. The arrows indicate areas of hepatic injury.

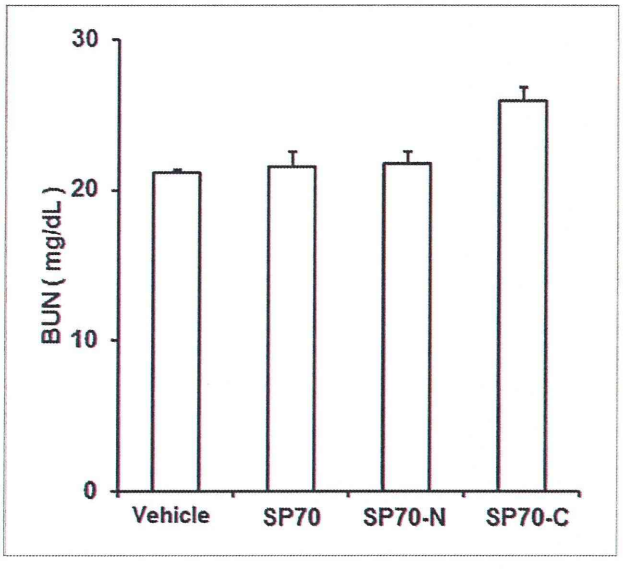

Fig. 3: Effect of SP70-N and SP70-C on kidney. SP70, SP70-N and SP70-C were intravenously administered at 40 mg/kg, 60 mg/kg, and 60 mg/kg, respectively. At 24 h after administration, blood was collected, and the resultant serum was used for the BUN assay with a commercially available kit. Data are means ± SEM (n = 4).

3.3. Biochemical analysis

Serum alanine aminotransferase (ALT) and blood urea nitrogen (BUN) were measured with commercially available kits according to the manufacturer's protocols (Wako Pure Chemical Industries, Osaka, Japan).

3.4. Histological analysis

The liver was excised and fixed with 4% paraformaldehyde. After sectioning, thin tissue sections of tissues were stained with hematoxylin and eosin for histological observation. Liver sections were stained with Azan-Mallory for observation of liver fibrosis.

3.5. Measurement of hydroxyproline content

Hepatic hydroxyproline (HYP) content was measured using Kivirikko's method (Kivirikko et al. 1967), with some modifications. Briefly, liver tissue (50 mg) was hydrolyzed in 6 mol/L HCl at 110 °C for 24 h in a glass test tube. After centrifugation at 3000 rpm for 10 min, 2 mL of the supernatant was neutralized with 8 N KOH. Two grams of KCl and 1 mL of 0.5 mol/L borate buffer were then added to the resultant solution, followed by incubation for 15 min at room temperature and a further incubation for 15 min at 0 °C. Freshly prepared chloramine-T solution was then added and the solution was incubated at 0 °C for 1 h, followed by the addition of 2 mL of 3.6 mol/L sodium thiosulfate. The samples were incubated at 120 °C for 30 min, and then 3 mL toluene was added with incubation for a further 20 min at room temperature. After centrifugation at 2000 rpm for 5 min, 2 mL of the supernatant was added to 0.8 mL of buffer containing Ehrlich's reagent and incubated for 30 min at room temperature. The samples were then transferred to a plastic tube and the absorbance was measured at 560 nm. Hydroxyproline content was expressed as micrograms of hydroxyproline per gram of liver.

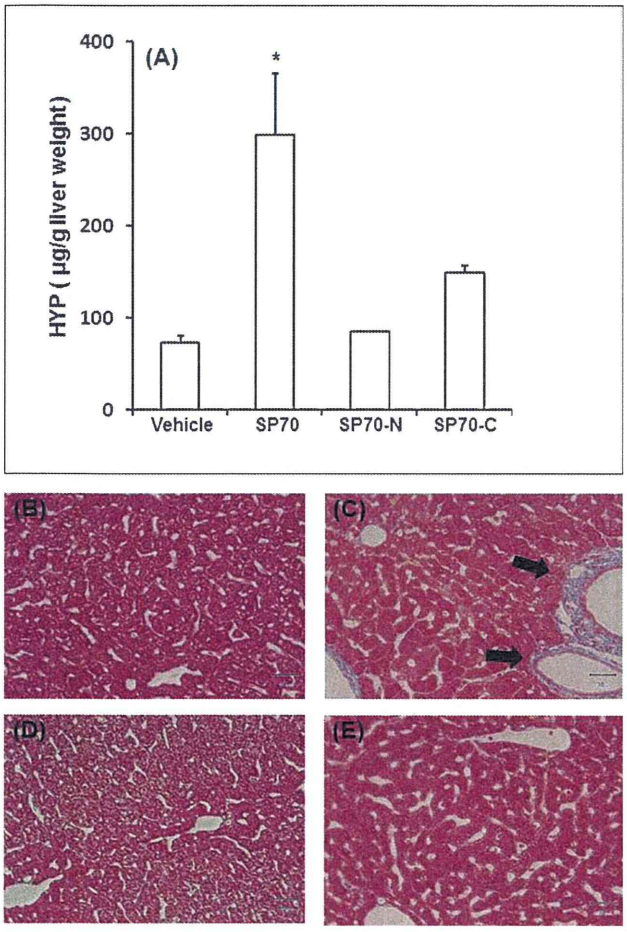

Fig. 4: Effect of SP70-N and SP70-C on chronic liver injury. SP70 was injected into mice every 3 days for 4 weeks at 30 mg/kg. SP70-C and SP70-N was injected into mice every 3 days for 4 weeks at 60 mg/kg. Three days after the last injection, the mice were sacrificed. Hydroxyproline levels (A) in the liver were measured. The liver was excised from mice treated with vehicle (B), SP70 (C), SP70-N (D) or SP70-C (E) and fixed with 4% paraformaldehyde. Tissue sections were stained with Azan and observed under a microscope. The arrows indicate areas of hepatic fibrosis. Data are means ± SEM (n = 4). *$p < 0.05$ as compared to the vehicle-treated group.

3.6. Statistical analysis

The data were analyzed for statistical significance using Dunnett's test. P values less than 0.05 were considered statistically significant.

References

Dobson J (2006) Magnetic micro- and nano-particle-based targeting for drug and gene delivery. Nanomed 1: 31–37.

Kim JS, Yoon TJ, Yu KN, Kim BG., Park SJ, Kim HW, Lee KH, Park SB, Lee JK, Cho MH (2006) Toxicity and tissue distribution of magnetic nanoparticles in mice. Toxicol Sci 89: 338–347.

Kivirikko KI, Laitinen O, Prockop DJ (1967) Modifications of a specific assay for hydroxyproline in urine. Anal Biochem 19: 249–255.

Lin YH, Mi FL, Chen CT, Chang WC, Peng SF, Liang HF, Sung HW (2007) Preparation and characterization of nanoparticles shelled with chitosan for oral insulin delivery. Biomacromolecules 8: 146–152.

Nishimori H, Kondoh M, Isoda K, Tsunoda S, Tsutsumi Y, Yagi K (2009a) Silica nanoparticles as hepatotoxicants. Eur J Pharm Biopharm 72: 496–501.

Nishimori H, Kondoh M, Isoda K, Tsunoda S, Tsutsumi Y, Yagi K (2009b) Histological analysis of 70-nm silica particles-induced chronic toxicity in mice. Eur J Pharm Biopharm 72: 626–629.

Oku N, Tokudome Y, Namba Y, Saito N, Endo M, Hasegawa Y, Kawai M, Tsukada H, Okada, S (1996) Effect of serum protein binding on real-time trafficking of liposomes with different charges analyzed by positron emission tomography. Biochim Biophys Acta 1280: 149–154.

Schiestel T, Brunner H, Tovar G.E (2004) Controlled surface functionalization of silica nanospheres by covalent conjugation reactions and preparation of high density streptavidin nanoparticles. J Nanosci Nanotechnol 4: 504–511.

Smith B, Wepasnick K, Schrote KE, Cho HH, Ball WP, Fairbrother DH (2009) Influence of surface oxides on the colloidal stability of multi-walled carbon nanotubes: a structure-property relationship. Langmuir 25: 9767–9776.

Warheit DB, Sayes CM, Reed KL, Swain KA (2008) Health effects related to nanoparticle exposures: environmental, health and safety considerations for assessing hazards and risks. Pharmacol Ther 120: 35–42.

Yoshida et al. Nanoscale Research Letters 2011, 6:195
http://www.nanoscalereslett.com/content/6/1/195

Nanoscale Research Letters
a SpringerOpen Journal

NANO EXPRESS Open Access

Promotion of allergic immune responses by intranasally-administrated nanosilica particles in mice

Tokuyuki Yoshida[1,2†], Yasuo Yoshioka[1,2,3*†], Maho Fujimura[1,2], Kohei Yamashita[1,2], Kazuma Higashisaka[1,2], Yuki Morishita[1,2], Hiroyuki Kayamuro[1,2], Hiromi Nabeshi[1,2], Kazuya Nagano[2], Yasuhiro Abe[2], Haruhiko Kamada[2,3], Shin-ichi Tsunoda[2,3,4], Norio Itoh[1], Tomoaki Yoshikawa[1,2], Yasuo Tsutsumi[1,2,3*]

Abstract

With the increase in use of nanomaterials, there is growing concern regarding their potential health risks. However, few studies have assessed the role of the different physical characteristics of nanomaterials in allergic responses. Here, we examined whether intranasally administered silica particles of various sizes have the capacity to promote allergic immune responses in mice. We used nanosilica particles with diameters of 30 or 70 nm (nSP30 or nSP70, respectively), and conventional micro-sized silica particles with diameters of 300 or 1000 nm (nSP300 or mSP1000, respectively). Mice were intranasally exposed to ovalbumin (OVA) plus each silica particle, and the levels of OVA-specific antibodies (Abs) in the plasma were determined. Intranasal exposure to OVA plus smaller nanosilica particles tended to induce a higher level of OVA-specific immunoglobulin (Ig) E, IgG and IgG1 Abs than did exposure to OVA plus larger silica particles. Splenocytes from mice exposed to OVA plus nSP30 secreted higher levels of Th2-type cytokines than mice exposed to OVA alone. Taken together, these results indicate that nanosilica particles can induce allergen-specific Th2-type allergic immune responses in vivo. This study provides the foundations for the establishment of safe and effective forms of nanosilica particles.

Introduction

With the recent development of nanotechnology, many nanomaterials with innovative functions have been developed. For example, nanoparticles of titanium dioxide and silica have been used in commercial applications related to medicine, cosmetics and food [1]. In particular, amorphous (noncrystalline) nanosilica particles possess extraordinary advantages, including straightforward synthesis, relatively low cost, and easy surface modification [1,2]. Nanosilica particles are increasingly being used for many applications, including cosmetics, food technology, medical diagnosis, cancer therapy, and drug delivery [1-4].

As the use of nanomaterials increases, there is rising concern regarding their potential health risks because there is preliminary evidence that the unique electrical and mechanical properties of nanomaterials is associated with undesirable biological interactions [5,6]. In addition, it has recently become evident that particle characteristics, including particle size and surface properties, are important factors in pathologic alterations and cellular responses [7-10]. For instance, Nishimori et al have previously demonstrated that nanosilica particles with relatively small particle size induce a greater level of toxicity, including liver injury, than do silica particles with larger particle size [11]. To create safe and effective forms of nanomaterials, studies which provide basic information regarding biological responses to nanomaterials are essential.

Numerous studies have shown that several types of nanomaterials increase the incidence of allergic immune diseases [12-14]. Activation of the Th2 response, including production of interleukin (IL)-4, IL-5, and IL-13 from Th2 cells (a subset of $CD4^+$ T cells) and immunoglobulin (Ig) G1 or IgE from B cells, is responsible for

* Correspondence: yasuo@phs.osaka-u.ac.jp; ytsutsumi@phs.osaka-u.ac.jp
† Contributed equally
[1]Department of Toxicology and Safety Science, Graduate School of Pharmaceutical Sciences, Osaka University, 1-6, Yamadaoka, Suita, Osaka 565-0871, Japan
Full list of author information is available at the end of the article

SpringerOpen
© 2011 Yoshida et al; licensee Springer. This is an Open Access article distributed under the terms of the Creative Commons Attribution License (http://creativecommons.org/licenses/by/2.0), which permits unrestricted use, distribution, and reproduction in any medium, provided the original work is properly cited.

many of the pathologic features of allergic immune diseases [15]. Some reports have shown that intranasal or airway exposure to nanomaterials promotes allergic immune responses, indicating the immune-activating potential of nanomaterials [12,13]. However, the role of the different physical characteristics of nanomaterials in the production of allergic responses has not been elucidated.

Here, we examined whether intranasal exposure to nanosilica particles has the capacity to promote allergic immune responses in mice. In addition, we investigated the relationship between the size of silica particles and allergic immune responses.

Materials and methods

Silica particles

Amorphous silica particles with a diameter of 30, 70, 300 and 1,000 nm (Micromod Partikeltechnologie, Rostock/Warnemünde, Germany, designated nSP30, nSP70, nSP300 and mSP1000, respectively) were used in this study. The particle numbers of silica particles were 3.5×10^{13}, 2.8×10^{12}, 3.5×10^{10}, or 9.5×10^{8} particles/mg (nSP30, nSP70, nSP300, or mSP1000, respectively). Silica particles were sonicated for 5 min and vortexed for 1 min before use. The size of particles was measured using a Zetasizer Nano-ZS (Malvern Instruments, UK). The mean size and the size distribution of particles were measured by means of dynamic light scattering. We confirmed that the particle size distributions of these silica particles were narrow.

Mice

Female BALB/c mice were purchased from Nippon SLC (Hamamatsu, Japan) and used at 6 to 8 weeks of age. All of the animal experimental procedures in this study were performed in accordance with the National Institute of Biomedical Innovation Guidelines for the Welfare of Animals.

Exposure protocols and detection of antigen-specific antibody responses by enzyme-linked immunosorbent assay

Female BALB/c mice were intranasally exposed to a 20 μL aliquot (10 μL per nostril) containing 10 μg of ovalbumin (OVA; Sigma Chemical Co, St. Louis, MO, USA) as antigen, plus nSP30, nSP70, nSP300, or mSP1000 at concentrations of 10, 50 or 250 μg/mouse, on days 0, 1, and 2. On day 21, plasma was collected to assess antigen-specific antibody (Ab) responses. Antigen-specific IgG and subclass IgG1 Ab levels were determined by enzyme-linked immunosorbent assay (ELISA). The ELISA plates (Maxisorp, type 96F; Nalge Nunc International, Naperville, IL, USA) were coated with 10 μg/ml OVA and incubated overnight at 4°C. Non-specific Ab binding was minimized by incubating the plates with 4% blocking solution (Block Ace; Dainippon Sumitomo Pharmaceuticals, Osaka, Japan) at 37°C for 2 h. Plasma dilutions were added to the antigen-coated plates and incubated at 37°C for a further 2 h. The coated plates were then washed with PBS containing 0.05% Tween 20 and incubated with a horseradish peroxidase-conjugated goat anti-mouse IgG solution (Southern Biotechnology Associates, Birmingham, AL, USA) at 37°C for 2 h. The color reaction was developed with tetramethylbenzidine (MOSS, Inc., Pasadena, MD, USA), stopped with 2N H_2SO_4, and quantitated by measuring OD_{450} minus OD_{655} using a microplate reader. OVA-specific IgE Ab levels in plasma were determined using commercial ELISA kits (Dainippon Sumitomo Pharma, Osaka, Japan).

Isolation of splenocytes

Spleens were aseptically removed and placed in RPMI 1640 medium (Wako Pure Chemical Industries, Osaka, Japan) supplemented with 10% fetal bovine serum, 50 mM 2-mercaptoethanol and 1% antibiotic cocktail (Nacalai Tesque, Kyoto, Japan). The single-cell suspension of splenocytes was treated with ammonium chloride to lyse the red blood cells, and the splenocytes were washed, counted, and suspended in RPMI medium supplemented with 10% fetal bovine serum, 50 mM 2-mercaptoethanol, 1% antibiotic cocktail, 10 mL/L of 100 × nonessential amino acids solution, 1 mM sodium pyruvate, and 10 mM HEPES to a final concentration of 1×10^{7} cells/mL.

Antigen-specific cytokine responses

Antigen-specific cytokine responses were evaluated by culturing the splenocytes (5×10^{6} cells/well) in the presence of OVA (1 mg/mL) in vitro. Cells were incubated at 37°C for 72 h. Culture supernatants from in vitro unstimulated and OVA-stimulated cells were analyzed by the Bio-Plex Multiplex Cytokine Assay (Bio-Rad Laboratories, Hercules, CA, USA) according to the manufacturer's instructions. The assay results were read on a Luminex 100 Multiplex Bio-Assay Analyzer (Luminex, Austin, TX, USA). The difference between the mean concentration of cytokines in supernatants from in vitro OVA-stimulated cells and unstimulated cells (background) was then calculated.

Statistical Analysis

All values are expressed as mean ± SEM. Differences between groups were assessed using analysis of variance followed by Turkey's method.

Results and discussion

Antigen-specific IgE Ab responses to silica particles

To assess the relationship between the size of silica particles and allergic immune responses, we used nanosilica

particles with diameters of 30 or 70 nm (nSP30 or nSP70, respectively), and conventional micro-sized silica particles with diameters of 300 or 1,000 nm (nSP300 or mSP1000, respectively). The mean secondary particle diameters of the silica particles measured by dynamic laser scatter analysis were 33, 79, 326, and 945 nm, respectively (data not shown). We examined the silica particles by transmission electron microscopy, and confirmed that they were well-dispersed smooth-surfaced spheres (data not shown). To investigate the potential of silica particles to enhance allergic immune responses, we examined their effect on the production of allergen-specific Abs responses in vivo. On days 0, 1, and 2, mice were intranasally exposed to OVA (10 μg/mouse) plus silica particles at concentrations of 10, 50, and 250 μg/mouse. On day 21, we collected plasma from the mice and performed an ELISA to examine anti-OVA IgE Ab responses. The levels of IgE Abs tended to be higher in mice exposed to OVA plus smaller nanosilica particles than in mice exposed to OVA plus larger silica particles (Figure 1a). In particular, the OVA-specific IgE Ab level in OVA plus nSP30-exposed mice was significantly higher than in mice exposed to OVA alone (Figure 1a). We consider that this level of IgE Ab would induce the mast cell degranulation and histamine release, which are major mechanisms underlying anaphylactic reactions in allergic diseases [16]. In addition, the OVA-specific IgE Ab response in mice exposed to OVA plus nSP30 increased in an nSP30-dose-dependent manner (Figure 1b). Taken together, these results suggest that nanosilica particles such as nSP30 are capable of inducing allergic immune responses and have the potential to cause serious allergic symptoms.

Antigen-specific IgG Abs subclass responses of silica particles

Next, to assess the types of immune responses elicited by silica particles, we measured the levels of anti-OVA IgG Ab and anti-OVA IgG1 Ab. IgG1 production is indicative of a Th2-type response. The levels of anti-OVA IgG and anti-OVA IgG1 Abs induced by intranasal-exposure to OVA plus smaller silica particles were higher than those induced by OVA plus larger silica particles (Figure 2); this was similar to the results observed for IgE Ab responses, described above (Figure 1). The levels of OVA-specific IgG Ab and OVA-specific IgG1 Ab in mice exposed to OVA plus nSP30 were significantly higher than in those exposed to OVA alone

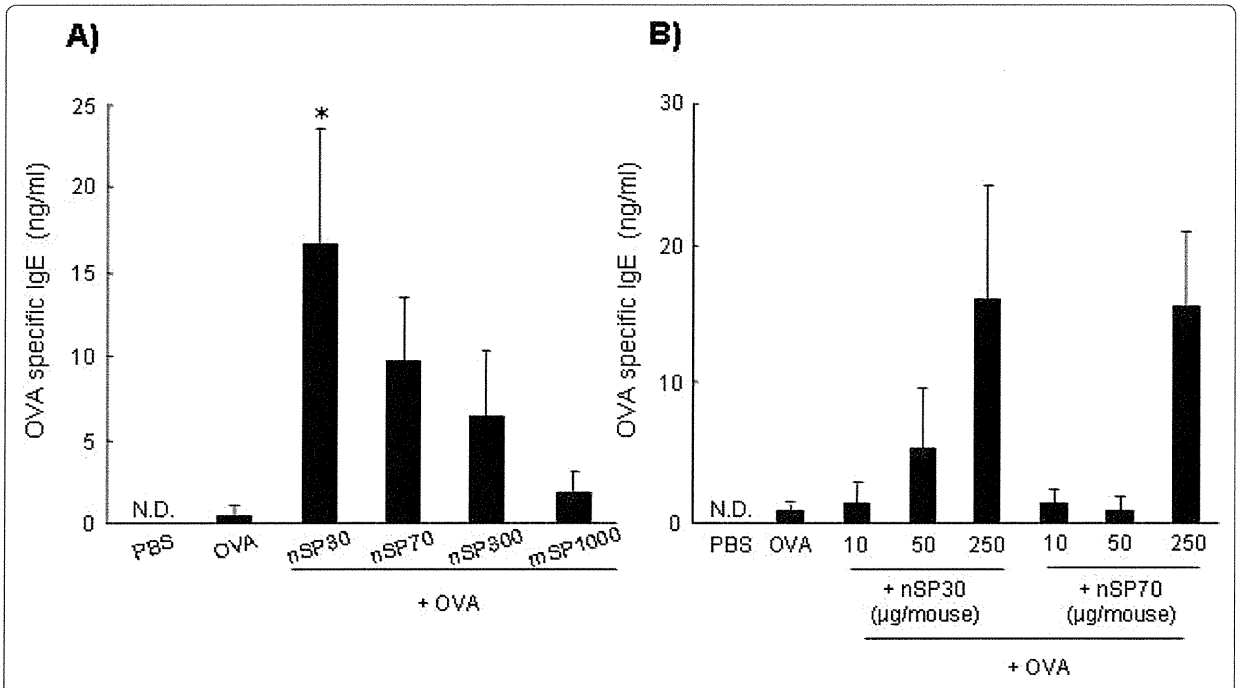

Figure 1 Plasma OVA-specific IgE Ab responses after intranasal exposure to OVA plus silica particles. **(a)** BALB/c mice were intranasally exposed to PBS (vehicle control), OVA alone or OVA plus silica particles (250 μg/mouse) on days 0, 1, and 2. **(b)** BALB/c mice were intranasally exposed to PBS (vehicle control), OVA alone or OVA plus the designated dose of nSP30 or nSP70 on days 0, 1, and 2. Plasma was collected on day 21 and analyzed by ELISA to assess (a) the relationship between silica particle size and OVA-specific IgE Ab responses and (b) the dose-response effect of nSP30 and nSP70 on OVA-specific IgE Ab levels. N.D., not detected. Data are presented as mean ± SEM (n = 8 to 13; *P < 0.05 *vs* OVA alone).